energies

MDPI

Review

Electrified Hydrogen Production from Methane for PEM Fuel Cells Feeding: A Review

Eugenio Meloni *, Giuseppina Iervolino, Concetta Ruocco, Simona Renda, Giovanni Festa, Marco Martino and Vincenzo Palma

Department of Industrial Engineering, University of Salerno, Via Giovanni Paolo II 132, 84084 Fisciano, Italy; giiervolino@unisa.it (G.I.); cruocco@unisa.it (C.R.); srenda@unisa.it (S.R.); gifesta@unisa.it (G.F.); mamartino@unisa.it (M.M.); vpalma@unisa.it (V.P.)
* Correspondence: emeloni@unisa.it

Abstract: The greatest challenge of our times is to identify low cost and environmentally friendly alternative energy sources to fossil fuels. From this point of view, the decarbonization of industrial chemical processes is fundamental and the use of hydrogen as an energy vector, usable by fuel cells, is strategic. It is possible to tackle the decarbonization of industrial chemical processes with the electrification of systems. The purpose of this review is to provide an overview of the latest research on the electrification of endothermic industrial chemical processes aimed at the production of H_2 from methane and its use for energy production through proton exchange membrane fuel cells (PEMFC). In particular, two main electrification methods are examined, microwave heating (MW) and resistive heating (Joule), aimed at transferring heat directly on the surface of the catalyst. For cases, the catalyst formulation and reactor configuration were analyzed and compared. The key aspects of the use of H_2 through PEM were also analyzed, highlighting the most used catalysts and their performance. With the information contained in this review, we want to give scientists and researchers the opportunity to compare, both in terms of reactor and energy efficiency, the different solutions proposed for the electrification of chemical processes available in the recent literature. In particular, through this review it is possible to identify the solutions that allow a possible scale-up of the electrified chemical process, imagining a distributed production of hydrogen and its consequent use with PEMs. As for PEMs, in the review it is possible to find interesting alternative solutions to platinum with the PGM (Platinum Group Metal) free-based catalysts, proposing the use of Fe or Co for PEM application.

Keywords: microwaves; process intensification; joule heating; PEM fuel cells; hydrogen

check for updates

Citation: Meloni, E.; Iervolino, G.; Ruocco, C.; Renda, S.; Festa, G.; Martino, M.; Palma, V. Electrified Hydrogen Production from Methane for PEM Fuel Cells Feeding: A Review. *Energies* **2022**, *15*, 3588. https://doi.org/10.3390/en15103588

Academic Editor: George Avgouropoulos

Received: 26 April 2022
Accepted: 12 May 2022
Published: 13 May 2022

Publisher's Note: MDPI stays neutral with regard to jurisdictional claims in published maps and institutional affiliations.

Copyright: © 2022 by the authors. Licensee MDPI, Basel, Switzerland. This article is an open access article distributed under the terms and conditions of the Creative Commons Attribution (CC BY) license (https://creativecommons.org/licenses/by/4.0/).

1. Introduction

It is clear that we need a new formula for the production of chemicals: the chemical processes still depend heavily on the intense heat generated by fossil fuels. Curbing carbon emissions, while maintaining quality of life, is a global challenge for manufacturing processes that will require process innovation. The decarbonization of energy-intensive manufacturing industries represents one of the most pressing technological challenges of the coming decades. Among these industries, the chemical sector (including refineries) is by far the most significant energy consumer [1]. One solution is to replace the energy produced by burning carbon-based fuels with energy from "green" sources such as electricity produced from renewable sources. From scientific literature it is possible to consider that, very often, the use of electricity is limited to the initial stages of the process such as the electrocatalytic conversion of water, CO_2 and/or nitrogen into hydrogen, carbon monoxide, syngas, formic acid, methanol or ammonia [2–5]. The subsequent reaction steps are usually carried out in the conventional way, therefore, by using the classical thermochemical path through the use of fossil fuels, especially in the case of endothermic reactions. However, if

the electrocatalytic production of fuels from water is certainly of fundamental importance to decarbonize the chemical sector, it is equally important to address the possible applications of electricity in subsequent reactions, which ultimately lead to thousands of products on the market today. Therefore, it is necessary to understand the role of electricity in chemical reactors and catalysts in order to identify the limits and advantages of this new technology. Electrification of conventionally fired chemical reactors has the potential to reduce CO_2 emissions and provide flexible and compact heat generation.

So, what are the possible approaches reported in the literature on the use of electricity for the development of chemical processes? Several techniques are possible: electrocatalytic or photoelectrochemical processes in which the direct supply of electric current (DC) to the electrodes results in the transfer of charge across the interface between the electrode and the treated liquid [6–8]; plasma reactors [9–11], in which highly reactive ionized gases (plasma) are generated through electricity, so resulting in large numbers of chemically active species, including electrons, ions, atoms and radicals [1]. Moreover, the transfer of thermal energy in electrified reactors can be achieved in various ways, such as: microwave-assisted heating, in which heat is generated through the displacement of dipolar molecules or ions in liquids caused by the rapidly alternating electric field of the microwaves; ohmic or Joule heating, in which heat is generated by an electric current passing through a resistive conductor; induction heating, in which heat is generated by eddy currents, resulting in the conductive materials by the rapidly alternating magnetic field, so resulting in the Joule heating of those materials [1]. The comparison among the different electrification methods is summarized in the following Table 1.

The role of electricity in chemical processes seems to be of particular importance for all those processes that we can define as endothermic, which require a supply of heat to develop the reaction and reach favorable thermodynamic equilibrium conditions to obtain the desired conversion and yield. In particular, electricity can be useful for providing heat to catalytic systems in a uniform way, avoiding thermal hot spots or large temperature gradients from the heat source towards the catalyst.

This is the case, for example, of processes such as reforming for the production of syngas, endothermic processes that require a constant supply of heat to the catalytic sites.

Industrial-scale reformers consist of hundreds of tubular reactors that need to be heated. Traditionally, heating occurs through the combustion of fossil fuels and the main mechanism of heat transfer is radiation. For this reason, to ensure the right amount of heat to the catalyst, combustion takes place at temperatures much higher than the actual reaction temperature. Energy losses are very high, as are fossil CO_2 emissions into the atmosphere.

Conventional reforming presents three main drawbacks [12]:

- Inefficient heat transfer. The heat for the reaction must first be transferred by radiation from the burning fuel to the outer walls of the reactor tube. Then, from the external wall, it must reach the inside of the pipe by conduction and finally reach the surface of the catalyst. Furthermore, generally the supports used for the catalysts are made of alumina, and therefore are poor thermal conductors.
- The maintenance costs of the reactor are relatively high. The high temperatures required stress the materials of which the pipes are made. Typically, a tube replacement is required after an average of 5 years of operation. Additionally, the costs for these interventions are very high, and can reach millions of dollars [12].
- Large quantities of methane (natural gas) are consumed in providing the heat energy for the reforming reaction. For example, a typical 1100 ton d^{-1} ammonia plant requires approximately 400,000 m^3 d^{-1} of natural gas only for the heating stage. While natural gas is a relatively cheap fuel today, it is a nonrenewable resource and may not remain cheap in the future.
- To supply thermal energy to the reforming reaction, it is necessary to burn large quantities of methane gas. Even though it is a relatively cheap fuel, it is nonetheless a fossil fuel and therefore not renewable.

Table 1. Comparison of different alternatives for the electrification of chemical reactors.

Mechanism	Principle	Pro	Cons
Ohmic or Joule	electric current passing through a resistive conductor produces heat ð, a conductive structured support (foam, monolith) is used on which the catalyst is deposited as thin film	- with respect to fired reactors and with electrically heated furnaces (in which the catalytic tubes are inserted), there is a minimization of transfer resistance and a solid–solid heat transfer (higher rate and efficiency) - catalysts have a shape different from conventional fixed/fluid/mobile bed applications, and should be optimized for the applications - avoidance also of mass transfer limitations, possible gradients between the catalyst and the gas phase (at lower T, beneficial to reduce side reactions)	- problems of adhesion and stability of the catalytic film over the structured support must be still solved - necessity for a specific redesign to optimize catalyst performance - possible side negative effect of structured substrate - examples of industrial development in the area are not available
Induction heating	rapidly alternating magnetic field either generates eddy currents in conducting materials, resulting in the Joule heating of those materials, or generates heat in ferro-/ferrimagnetic materials by the magnetic hysteresis losses	- studied in literature, known for over 70 years, but scarcely applied to catalytic reactors - used in some industrial applications (fast preheating of petroleum fractions - simple design, possible induction oscillations - localized heating at the catalyst, creation of thermal gradients with the flowing gas phase (rapid quench) - technology available industrially for other applications	- need to add a component which can be heated by induction - possible alternations in stability, selectivity, potential decrease productivity - possible interferences with integrated Pd membrane
Microwave/RF heating	rapidly alternating electric field of the microwave generates heat by moving dipolar molecules or ions in liquids, or by getting absorbed in the so-called "dielectric lossy" solid nonmagnetic materials	industrial experience for fine chemicals production relatively simple technology	effective with liquids, less with gas reactions; main challenge with heterogeneous catalysts to achieve uniform heating; proposed solutions difficult to scale-up

In the literature, there are several research studies aimed at improving the energy efficiency of these processes that promote their sustainability. The catalysts currently used in the industrial sector consist of alumina pellets which, having a low coefficient of thermal conductivity, offer considerable resistance to the passage of heat [13]. From the studies, it emerged that the choice of structured catalysts prepared, starting from carriers with high thermal conductivity, such as silicon carbide, either in monolithic form [14] or in the configuration of heating element [15], or conductive foams in which the pores are filled with the catalyst [16], allows to optimize the system from a thermal point of view, ensuring a more homogeneous radial thermal profile and, therefore, a reduction of hotspots phenomena [17].

With a view to intensifying chemical processes, different electrification technologies are being developed. Thanks to the use of renewable sources, they will be able to support the environmental cause and also to improve the efficiency of the process itself, such as the thermal transfer.

For this purpose, there are several systems aimed at supplying thermal energy, starting from electrified solutions, which are proposed in the following paragraphs.

In particular, this review was focused on the electrification of the methane reforming processes, in which the heating was obtained by microwave irradiation and the Joule effect. The produced streams, after further purification stages (not in the scope of the review), for example, by means of a membrane for obtaining H_2 with the desired purity, may be used for feeding fuel cells for more sustainable and in situ energy production. Among the others, the PEM fuel cells have been chosen for this review.

2. Microwaves

Microwaves, which can be produced from the electricity obtained from renewable energy sources, can be effectively used for heating chemical reactors, which are currently conducted by using the burning of fossil fuels, thus helping in the chemical industry's electrification [18]. Apart from its peculiar characteristics (rapid, volumetric and selective), the microwave heating can result in a huge process intensification, since it may allow an improvement in at least one of the main process parameters, such as yield, selectivity, capital or operating cost, as well as may reduce the environmental impact of a process. In recent years, microwave heating has successfully been applied in commercial fields, including food processing, physical and chemical treatments of wood, plastic, rubber and ceramics [19]. Regarding the application of microwave heating to chemical engineering processes, some main issues must be further investigated [20]. In the last decade, several research efforts have been focused in this direction, with several groups investigating the possibility to intensify some chemical processes, such as ammonia production at low pressure [21] and methane and biomass valorization [22,23], through the use of the MW heating. These recent studies evidenced interesting results and pose the basis for further research. One of the main features of most industrial chemical reactors is that they have (i) a fixed bed, (ii) a fluidized bed, (iii) slurry or (iv) a monolithic configuration, thus being multiphase. The MW heating, being selective (microwaves may preferentially heat a phase or material with respect to others), may have a fundamental importance in multiphase reactors. For example, in a silicon carbide (SiC) monolith, the selective heating realized, since only the solid absorbs microwaves (so heating itself), may cause a temperature difference between the hot solid and the cold gas present in its channels, therefore influencing the homogeneous and heterogeneous reactions inside the reactor. This behavior is peculiar for the microwave heating of multiphase reactors and cannot be obtained in conventional heating [24]. Selective heating can also result in highly localized heating or hot spot formation [25], sometimes related to arcing or plasma [26], which can occur in the case of the concentration of the electric field in a small gap between microwave absorbers, such as activated carbon and silicon carbide [27,28]. So, arcing or plasma occurs when the electric field strength becomes higher than the dielectric strength of the continuum phase (~3 MV/m for air) [29]. Sharp edges and other surface irregularities, allowing the accumulation of free charges with a consequent increase in the charge density and the resulting electric field, may help arc formation [28,29]. The occurrence of hot spots in multiphase reactors can be productive [30,31] or deleterious [32]. In fact, hot spots can either reduce the catalyst activity by promoting, for example, the crystallization of the metal nanoparticles dispersed on it [33,34], or the localized higher temperature may result in enhanced reaction performance by obtaining (i) higher temperatures for the heterogeneous reactions to occur [35,36] or (ii) the desorption of the products from the catalyst surface at a higher rate [37]. In the past decade, several research groups have focused their attention on microwave multiphase reactors, such as monoliths [23,37–41], fixed beds [42–45] and slurry reactors [33–35]. Applications of these studies include polymerization [46], biomass valorization [47,48], epoxidation [49,50], methane nonoxidative coupling [23], methane steam reforming [39], MW-assisted CO_2 desorption from zeolites 13X [45] and propane dehydrogenation [41]. The studies evidenced the effective process intensification obtained through MW heating, since higher yields and selectivity, as well as lower processing time, have been shown. One of the main issues still remaining is the accurate measurement of the temperature in MW-assisted processes; in this sense, only in few cases [23,38,40] have

the temperatures of the different phases been reported with sufficient spatial resolution. Some reviews have been published in the recent past, either dealing with specific areas of chemical engineering [51] or providing a broad overview of the applications of microwave heating in chemical engineering processes [52,53].

In this review, reactions have been chosen as an example of chemical processes intensified by applying MWs. In the following subsections, the most recent advances in MW-assisted catalytic methane reforming reactions are shown, by also focusing on the reactor design.

2.1. MW-Assisted Reforming

Three different routes for methane reforming are widely known:

1. Steam reforming of methane, SRM, Equation (1), developed for the first time by Sabatier and Senderens in 1902 [51];
2. Dry reforming of methane, DRM, Equation (2), which was studied for the first time by Fischer and Tropsch in 1928 over cobalt and nickel catalysts [54], and then optimized in 1948 by Reitmeier et al. [55], in whose studies the presence of steam into DRM feeding stream resulted in suppressing coke formation;
3. Partial oxidation of methane, POM, Equation (3), studied for the first time in 1949 by Lewis et al. [56], whose studies were performed by reforming methane through oxidizing it with oxygen using supported copper oxide catalyst.

$$\text{SRM: } CH_4 + H_2O \rightleftharpoons 3H_2 + CO \ \Delta H^0{}_{298K} = +206.1 \text{ kJ mol}^{-1} \quad (1)$$

$$\text{DRM: } CH_4 + CO_2 \rightleftharpoons 2H_2 + 2CO \ \Delta H^0{}_{298K} = +247 \text{ kJ mol}^{-1} \quad (2)$$

$$\text{POM: } CH_4 + 1/2\ O_2 \rightleftharpoons 2H_2 + CO \ \Delta H^0{}_{298K} = -36 \text{ kJ mol}^{-1} \quad (3)$$

As evident from the above reported equations, SRM and DRM are highly endothermic reactions, while POM is a slightly exothermic one [57]. Each of the three mentioned reforming processes has its peculiarities, resulting in pros and cons in the adoption of a process with respect to the others. In fact, for example, the Fischer–Tropsch (FT) process can be used for the synthesis of oxygen-containing chemicals by using the syngas with a H_2:CO ratio higher than two produced by SRM [58], while the use of the syngas with a H_2:CO ratio near to one produced by DRM increases the selectivity of long chain hydrocarbons during the same FT process [59]. In addition, the reduced energy input needed for POM, due to its exothermicity, could probably make it more attractive, even if it requires high purity oxygen feed, with a consequent need for safety control auxiliaries and high operating cost. SRM and DRM are generally performed at temperatures higher than 800 °C by using heterogeneous catalysts to achieve high methane conversion [60,61]. Different studies present in the literature have shown that DRM and SRM processes can be performed at temperatures in the range 400–500 °C over highly active Ni-based catalysts [62–64], but a methane conversion lower than 20% has been reported. Several studies have also proposed the combination of different reforming processes aimed at eliminating/reducing the drawback of a particular reforming process. For example, the combination of an exothermic and an endothermic reaction can result in a decreased high purity oxygen requirement in the reactor, as well as in enhanced thermal efficiency by exchanging heat from the different reactions [18]. On the other hand, the combination of DRM and SRM can allow the presence of the gasification reaction between coke and water on the catalyst surface (Equation (4)), which can (i) help in reducing the coke formation and deposition issue and (ii) increasing the H_2:CO ratio [65].

$$C + H_2O \rightleftharpoons CO + H_2, \qquad \Delta H^0{}_{298K} = -131 \text{ kJ mol}^{-1} \quad (4)$$

In the three mentioned reforming reactions performed by using conventional heating, four steps, below summarized, have been reported in the presence of a heterogeneous catalyst [66]:

(i) The first step, considered as the rate-determining one, is the methane activation. The energy needed for the rupture of C-H_x or CH_x-H_x bonds is governed by the surface properties. Each partially dissociated CH_x species is adsorbed on the catalyst surface, which sees also the presence of active carbonaceous species, C*.

(ii) The second step is the activation of coreactants (H_2O, CO_2, or O_2), whose absorption and dissociation on the catalyst surface or metal–support interface results in the formation of active oxygen species.

(iii) The third step is the formation of the O-H group: the reaction between CO_x and H radicals or surface O and H radicals allows the formation of surface hydroxyl (OH-) groups. The interaction of the adsorbed CH_x species and the O-H groups results in the formation of CH_xO intermediates, which then decompose to CO and H_2. The catalyst–support interface normally serves as an active site for CH_xO formation.

(iv) The fourth step is the oxidation and desorption of intermediates: the oxygen species on the metal catalyst surface may react with a surface group (CH_x group, CH_xO or $CO_{surface}$). Consequently, the formation of CO through the dissociation of CH_xO and $CO_{surface}$ or the Boudouard reaction (Equation (5)) may be obtained. Other side reactions affecting the overall reforming performance and product selectivity may occur, including reverse water gas shift (Equation (6)), and CH_4 decomposition shift (Equation (7)) [66].

$$CO_2 + C^* \rightleftharpoons 2CO, \qquad \Delta H^0{}_{298K} = +172 \text{ kJ mol}^{-1} \tag{5}$$

$$CO_2 + H_2 \rightleftharpoons CO_{surface} + H_2O, \qquad \Delta H^0{}_{298K} = +41 \text{ kJ mol}^{-1} \tag{6}$$

$$CH_4 \rightleftharpoons C^* + H_2, \qquad \Delta H^0{}_{298K} = +75 \text{ kJ mol}^{-1} \tag{7}$$

Our literature review evidenced that the reaction routes occurring in catalytic MW-assisted methane reforming seems to be like the ones of conventional methane reforming, with enhanced performance in the former case, mainly due to two peculiar effects: (i) thermal and (ii) specific or nonthermal. These two effects are briefly summarized in the following lines.

Thermal effects due to MW irradiation are generally associated with the hot spot formation and selective heating, considered, as previously mentioned, the main responsible in the increased reactant conversion and product selectivity in the gas phase reaction. In fact, in the case of reforming reactions, the localized higher temperatures may result in an easy activation of adsorbed CH_4 and coreactants (O_2, CO_2, or H_2O), with the consequent formation of syngas [39,65]. As a rule, the thermal effects are mainly related to the ability of the catalyst to absorb the MW irradiation.

In contrast, the nonthermal effects are due to physical interaction between gaseous molecules and MWs, but this point is still under debate from the scientific community, in which conflicting opinions from several theoretical and experimental studies are present. Regarding this aspect, several review papers discussing on this subject are available, which can be consulted by interested readers [66,67]. In general, in some studies the hypothesis that the coupling of MW energy and gaseous molecules may occur, so resulting in the population of the quantum vibration state, which is defined as the rotational excited state to promote gaseous molecules' dissociation. Following such a mechanism, the reduction of the Arrhenius activation energy for the dissociation of gaseous molecules can be obtained, as demonstrated by some recent studies in which the catalytic MW-assisted decomposition of NO to N_2 and O_2 has been investigated [68,69]. In addition, some recent studies have been able to attribute the enhanced performance in MW-assisted reactions to nonthermal effects, through the use of advanced measurement techniques such as in the real time Raman spectroscopy measurement equipped with fiber optic thermometer [70–72]. More deep discussions on the nonthermal effects of MWs are present in the works of Stuerga and Gaillard [73,74]. Other studies are present which use fixed bed reactors and that have argued that the nonthermal effects resulted in the reduction of the activation energy of the studied reactions [75–77]. In any case, in these studies, differently from the previously

mentioned ones, the temperature of the systems was measured through infrared pyrometer or thermocouples, and therefore with a nonaccurate spatial resolution: so, definitive evidence is difficult to find.

2.2. MW Reactors

One of the main challenges in the development of microwave heating-based technologies is the proper design of the microwave cavity, in particular with the aim to scale-up a MW-assisted reactor. In fact, the sensitive nature of the standing wave pattern of the electric and magnetic fields and the ineffective heating of the reactor due to the penetration depth becoming smaller than the reactor size make this step very difficult. Therefore, these drawbacks must be overcome for a widespread application of MW heating in chemical processes. In this sense, the fast progress in computational resources and the availability of user-friendly multiphysics commercial software could be helpful, for example, in providing the exact distribution of the 3D temperature and electromagnetic field in a microwave cavity and reactor [78]. However, progress in CFD goes on slowly with respect to the advances in experimental tests. In fact, the presence of different aspects which must be considered makes the modeling of microwave multiphase reactors very challenging, aspects which are related to the peculiar nature of the reactors, simultaneously being multiphase (they are characterized by the presence of more than one phase, such as gas and solid or gas and liquid), multiphysics (they are characterized by the presence of different physics, such as electromagnetism, transport processes and chemical reactions) and multiscale (they are characterized by a variable length scale, from a single catalyst particle to the microwave cavity). Due to these difficulties, few comparative studies are present in which the simulation results are validated with experimental tests [79–83]. In any case, the majority of these studies have been performed considering only single-phase systems, such as the microwave heating of liquids in a glass vial [79,80,83]. In the case of multiphase systems, several simplifications are needed to effectively manage the complexity of the system and obtain the results in a reduced computational cost. For example, some studies are available in which a multiphase fixed bed reactor, constituted by uniformly arranged large particles [43], biphasic solid hydride [84] and zeolites [45,85], was considered a continuum, and in the simulations the experimentally measured effective permittivity of the sample was employed. However, these simplifications should be carefully chosen, since they can introduce large uncertainties in the model predictions, which can result in uncertainties for the reactor design.

In this review, the attention was focused on multiphase reactors, which in general can be classified as fluid–fluid (which in turn are divided into dispersed and biphasic) and fluid–solid (which in turn are divided into slurry, fixed bed and structured bed), depending on the phases involved. In the following subsections, more details are reported regarding the recent studies on the MW-assisted heating of multiphase reactors, also giving an outlook on the challenges and opportunities in achieving an effective process intensification driven by microwaves.

2.2.1. Fluid–Fluid Systems

The most typical fluid–fluid systems are composed by two immiscible fluids which, being in contact with each other, are selectively heated by MWs depending by their different dielectric properties. As shown in Figure 1, the fluid–fluid systems can be either dispersed (one phase can be dispersed in the other), usually used in the emulsion polymerization of various monomers [86–88], or biphasic (two bulk phases with the formation of a single interface), usually used for reactive extraction applications [89–91], such as in biomass conversion. In the former case, the rate and product distribution of emulsion polymerization is sensitive to the dielectric properties of monomers and solvents, which must be properly chosen. In the latter case, the different dielectric properties of the two bulk immiscible liquids may allow the formation of a temperature gradient between them when exposed to the MW field. The characteristic selective heating of one phase obtained by using MWs,

coupled to the solubility of the solute depending on temperature, can play a crucial role in reactive extraction.

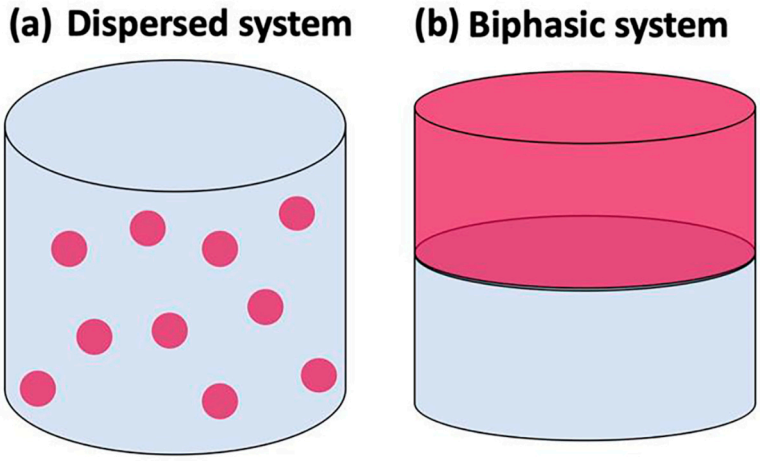

Figure 1. Schematic of the two extreme mixing cases of fluid–fluid systems. (**a**) Dispersed system; (**b**) Biphasic system. Reprinted from [18].

2.2.2. Fluid–Solid Systems

The fluid–solid systems represent the main part of the applications of microwave heating in multiphase systems, with a particular attention on heterogeneous catalytic reactors, which, as known, play an essential role across the chemical industry. As mentioned in the previous section, selective MW heating may result in increased reactant conversion with reduced reaction time. Moreover, the presence of a temperature gradient with a "hot" solid catalyst and a "cold" fluid due to MW irradiation may be helpful in limiting/avoiding the homogeneous gas phase reactions, so resulting in higher selectivity to the desired products if compared to conventional heating. In the fluid–solid systems, the three different reactor configurations shown in Figure 2 are usually employed, addressed as (a) slurry, (b) fixed bed and (c) structured bed reactors.

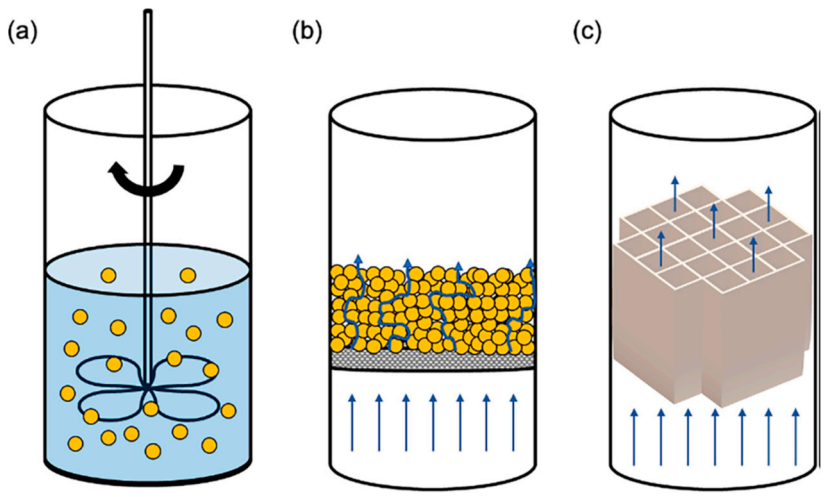

Figure 2. Three major categories of solid–fluid reactors utilized in microwave heating: (**a**) Slurry reactor; (**b**) Fixed bed reactor; (**c**) Structured bed reactor. Reprinted from [18].

The attention of the authors is focused to structured reactors, whose peculiar properties can allow to overcome some disadvantages of the fixed bed ones. In fact, the use of structured reactors (Figure 2c) instead of fixed bed ones may result in (i) more uniform temperature distribution, (ii) lower hot spot formation, (iii) decreased pressure drop and (iv)

better heat and mass transfer rates [92] due to their higher heat conduction properties compared to fixed beds [93]. In the MW-assisted reactions, the most used structured catalysts are in the monolith and open-cell foam configuration, made of silicon carbide or cordierite. The former material has a well-known high thermal conductivity (up to 400 W m^{-1} K^{-1}) and is a very good microwave absorber ($\varepsilon r = 9.72 - 2.01j$); in contrast, the latter material has both a low thermal conductivity and MW susceptivity (up to 3 W m^{-1} K^{-1} and $\varepsilon r = 1.5 - 0.007j$, respectively). For these reasons, the use of a structured catalyst prepared on a cordierite support in a MW-assisted reaction strongly depends on the dielectric properties of the catalyst coating. For example, the increase in the loss tangent of a cordierite monolith from 0.004 to 0.020 may be obtained after coating it with a silver–copper oxide (tan $\delta e = 1.029$) catalyst [94]. In addition, the uniformity of the catalyst coating is mandatory for a successful MW-assisted process when using cordierite: in fact, the presence of a thicker catalyst coating results in hot spot formation due to preferential heating. In this way, a boost of reactivity is obtained, with a consequent inhomogeneous accumulation of side products, such as coke (its presence is detrimental for the microwave field leading to microwave decoupling). In the case of SiC monoliths, a more uniform temperature profile can be obtained even with an irregular catalyst coating [95].

In recent years, different experimental investigations have been performed aimed at demonstrating that an effective process intensification in terms of selectivity to the desired product and production rate may be possible by using MW-heated structured reactors. In these studies, the selective heating of the solid with respect to the gas phase led to a clear temperature difference between the two phases, with the solid having a higher value. Therefore, a higher catalytic reaction rate and the suppression of the gas-phase side reactions were obtained, so resulting in a significant intensification of yield and selectivity. At present, SiC-based monoliths are ideal material for developing structured reactors. However, the research of new and innovative materials with nonconventional geometries could be helpful in increase the availability of structured reactors. Their peculiar properties make the structured reactors usable in different MW-assisted processes, not only chemical transformations, including also, for example, hydrogen release from metal hydrides [96].

Most of the studies in the literature focused on fluid–solid systems in which the fluid is a gas. Some examples are also present in which liquids are fed to structured reactors, such as in the case of the MW-assisted degradation of malachite green (an organic pollutant), by using $CoFe_2O_4$/SiC foam [97].

The reforming reactions belong to the gas–solid multiphase reactors, and in the following Table 2, a summary of the performance of the most recently developed catalysts in the MW-assisted ones is given.

Table 2. Summary of the performance of the most recent developed catalysts in MW-assisted reforming processes.

Process	Catalyst	MW Input	Operating Condition	X_{CH4}; X_{CO2}	Energy Consumption kWh $Nm^{-3}H_2$	Reference
DRM	Ni/Al_2O_3	P = 45–60 W	CO_2/CH_4 = 1 T = 800 °C WHSV = 11,000 mL g^{-1} h^{-1}	XCH_4 = 90% XCO_2 = 90%	-	[58]
DRM	Pt/C	P = 45–60 W	CO_2/CH_4 = 1 T = 800 °C WHSV = 11,000 mL g^{-1} h^{-1}	XCH_4 = 90% XCO_2 = 90%	-	[58]

Table 2. *Cont.*

Process	Catalyst	MW Input	Operating Condition	X_{CH4}; X_{CO2}	Energy Consumption kWh $Nm^{-3}H_2$	Reference
DRM	Ni/Al_2O_3-SiC	P = 45–60 W	CO_2/CH_4 = 1 T = 800 °C WHSV = 11,000 mL g^{-1} h^{-1}	XCH_4 = 90% XCO_2 = 90%	-	[58]
DRM	Ni/SiC	P = 45–60 W	CO_2/CH_4 = 1 T = 800 °C WHSV = 11,000 mL g^{-1} h^{-1}	XCH_4 = 90% XCO_2 = 90%	-	[58]
DRM	$7Ru/SrTiO_3$	P = 36.99 kW	CO_2/CH_4 = 1 T = 940 °C.	XCH_4 = 99.5% XCO_2 = 94%	18.58	[98]
DRM	Fe/HZSM-5	P = 700 W	CO_2/CH_4 = 1 WHSV = 2.4 L h^{-1} g^{-1}	XCH_4 = 63.03% XCO_2 = 91.27%	-	[24]
DRM	$La_xSr_{2-x}CoO_4$-Mn	P = 140 W	CO_2/CH_4 = 1 WHSV = 10 L h^{-1} g^{-1}	XCH_4 = 80% XCO_2 = 80%	3.98	[99]
DRM	Co-Mo/TiO_2	P = 100 W	CO_2/CH_4 = 1 WHSV = 10 L h^{-1} g^{-1}	XCH_4 = 81% XCO_2 = 86%	-	[100]
DRM	Cu-Mo/TiO_2	P = 100 W	CO_2/CH_4 = 1 WHSV = 10 L h^{-1} g^{-1}	XCH_4 = 76% XCO_2 = 62%	-	[100]
DRM	Ni-Co/ZrO_2-CaO + SiC	-	CO_2/CH_4 = 1 WHSV = 10 L h^{-1} g^{-1} T = 800 °C	XCH_4 = 97.1% XCO_2 = 99.2%	-	[101]
DRM	10Ni/AC	-	CO_2/CH_4 = 1 WHSV = 33 L h^{-1} g^{-1} T = 650 °C	XCH_4 = 48% XCO_2 = 51%	-	[102]
DRM	Ni/MgO/AC	-	CO_2/CH_4 = 1 WHSV = 33 L h^{-1} g^{-1} T = 650 °C	XCH_4 = 82% XCO_2 = 85%	-	[102]
SRM	15%Ni/CeO_2- Al_2O_3 on a SiC monolith	P = 800 W @ GHSV = 3300 h^{-1} P = 1000 W @ GHSV = 5000 h^{-1}	GHSV = 3300 and 5000 h^{-1} T = 550–950 °C P = 1 bar S/C = 3	CH_4 equilibrium conversion T = 800 °C—GHSV = 3300 h^{-1} T = 850 °C—GHSV = 5000 h^{-1}	3.8	[39]

2.3. Remarks

The literature survey and the consequent discussions reported in the above subsections revealed that the higher performance of the MW-assisted catalytic reforming reactions compared to the conventional ones are attributed to both thermal and nonthermal effects. More detailed fundamental investigations are, however, required to better explain and unravel the role of the latter. A future direction for improving the knowledge, and a wider use of the MW-assisted processes, is the better understanding of how to tune the solid–fluid temperature difference as a function of the operating conditions and materials. In this sense, the very recent introduction of fixed bed micromonoliths could introduce some advantages, such as the improvement of catalyst loading, thereby allowing flexibility in material selection and the avoidance of hot spots formation [103]. Moreover, additive manufacturing, enabling the production of complex structures, could be effectively employed in the future years for the development of microwave-heated reactors.

3. Electrical Resistive (Joule) Heating

Another technology for the supply of heat through electricity is ohmic or Joule heating, using those called "Resistance-heated reactors" [1]. In this regard, an interesting concept was presented in a recent article by Wismann et al., which proposed a new electric reactor heated by the Joule effect for the steam reforming of methane [104].

In their article, they describe how to integrate the electrically heated catalyst directly into a steam reformer to produce hydrogen. With this reactor and catalytic configuration, there is an intimate contact between the electrical heat source and the reaction site on the catalyst, which favors the achievement of thermodynamic equilibrium conditions and reduces the formation of byproducts. In detail, Wismann et al. propose an experimental reformer heated by the Joule effect, consisting of tubes made of Fe-Cr-Al alloys inside which the reaction takes place, for which the heat is supplied by direct electric current applied to the reactor through connectors of electrical copper. On the internal surface of the tubes, a layer of zirconia washcoat is present, and nickel has been deposited as an active species. The most important advantage of this type of reactor lies in the significantly smaller radial temperature gradients obtained with a thin catalyst layer on the tube wall, which is heated by the Joule effect, compared to a conventional method of a heated tube containing a fixed bed of catalyst pellets. They have also evidenced that an electrified compact reactor can be designed with overall dimensions potentially 100 times smaller than conventional ones [105]. Below is a figure extracted from the work of Wismann et al. representing the system described (Figure 3).

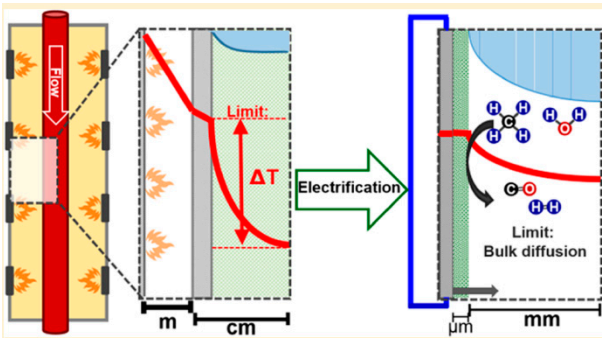

(**a**) (**b**)

Figure 3. Electrified compact reactor with temperature profile on catalyst surface with thermal heating (**a**) and electrical heating (**b**). Reprinted from [104].

An interesting study concerns the endothermic reaction of DRM, in which metal catalysts supported on La-ZrO_2 were used [106]. In particular, the catalytic activity was examined in the presence of an electric field generated by two stainless electrodes inserted inside the reactor, with each end connected as a contact to the catalyst bed. The results showed that with the application of the electric field, with a current of 3 mA, it is possible to appreciate an activity even at 523 K, already having a CH_4 conversion of 5%. The electric field acts on the reaction rate by promoting the dissociative adsorption of CH_4 on the surface of the catalyst. In addition, the possibility of working at "low temperatures" compared to the traditional DRM determines the achievement of high selectivity, high H_2/CO ratios and, in particular, low coke deposition. A schematic representation of electrified catalyst used in this study is reported below (Figure 4).

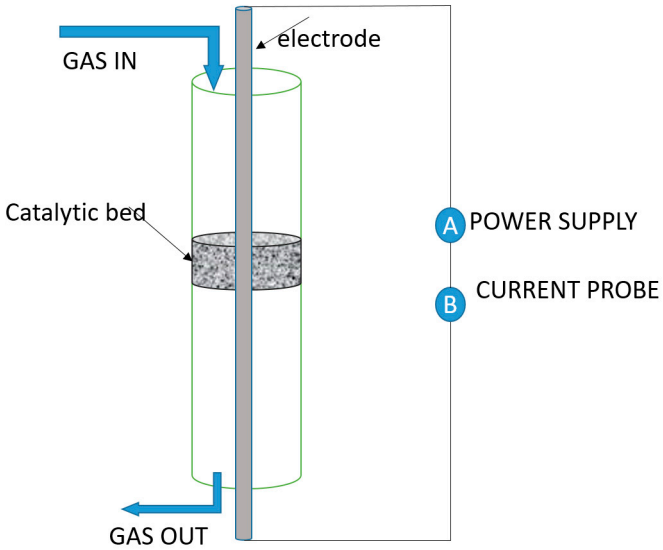

Figure 4. Schematic representation of the experimental setup and electrified catalyst. Adapted from [106].

Rieks M. et al. [107] developed an electrically heated reformer for dry and steam reforming reactions. They use a reactor with an internal electrical resistance heating, with an axial structure consisting of FeCrAl alloy elements coated with a catalytic layer of $LaNi_xRu_yO_z$ and connected to an electrical power source. In order to define the optimal reaction conditions during the experiment, different parameters were evaluated. The experimental tests were carried out in a range of 750–900 °C and, as expected, as the temperature increases, the conversion of CH_4 also increases. However, this effect is reduced at a temperature of 900 °C. The increase in the CO_2/CH_4 ratio in the 1.5–3 range, keeping the CH_4 partial pressure constant, leads to a lowering of the reaction rate: this effect was explained through the difficulty of CH_4 to adsorb itself on the surface of the catalyst. Interesting experiments were conducted with heating elements covered with different catalyst amounts. The results demonstrate that the reaction rate was strongly influenced by the catalytic load, showing again the influence of internal diffusion, leading to a decrease of the catalyst effectiveness for thicker washcoat layers. In this reactor configuration, the catalyst is the origin of the reactor heating: this reduces the problems related to heat transfer that are typically faced in externally heated reactors [107].

Spagnolo et al. [12] studied the electro-steam reforming of methane on a metal screen washcoated with Ni/Al_2O_3 and demonstrated energy efficiency compared to the traditional process. The authors proposed a novel approach to steam reforming where the principle of resistive heating (due to the use of electrical energy) was used for supplying heat directly to the catalyst surface. In their work, the catalyst was prepared starting from a resistant metal screen used as support, which was covered first with a washcoat of alumina and then with nickel as the active species. The reactor consisted of a relatively large diameter (1–2 m) ceramic-lined pressure vessel, in which properly designed and realized feedthrough terminals were used for the connection of the two sides (upper and lower) to an AC supply.

Specifically, the catalyst proposed by Spagnolo et al. consisted of various corrugated steel sheets, coated with a layer of gamma alumina (14%) and nickel (9.5%), rolled up on themselves [12].

Below is a schematic of the reactor configuration proposed by the authors (Figure 5):

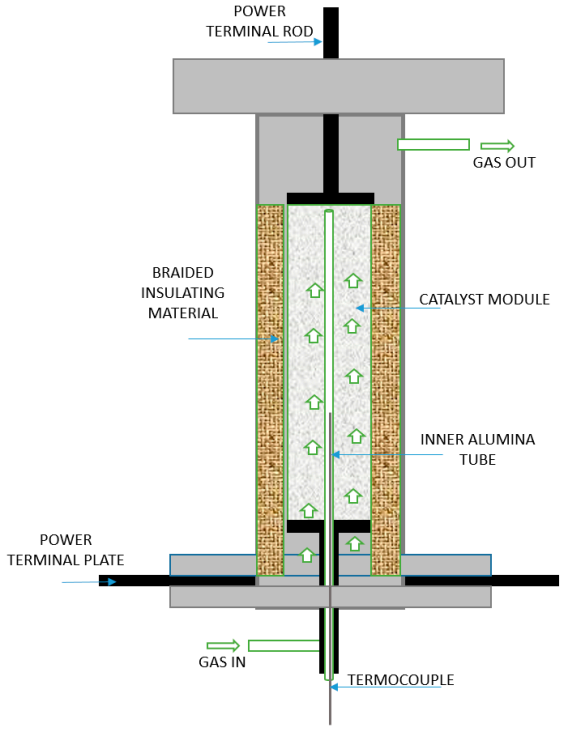

Figure 5. Schematic diagram of catalytic electrified reactor. Adapted from [12].

The performance of this catalyst was evaluated both in terms of CH_4 conversion and as energy required to produce hydrogen. The electrical energy (ER) required to produce hydrogen expressed in [kJ L^{-1} of produced H_2] is given by:

$$ER = 6 \times 10^4 \frac{E_{IN}}{F_M CE_n} \tag{8}$$

where CE is the conversion efficiency, calculated as:

$$CE = 1 - \frac{CH_4}{CH_4 + CO + CO_2} \tag{9}$$

E_{in} is the electrical energy input to the catalyst in kW, F_M is the inlet methane flow in mL min^{-1} and n is the molar ratio of H_2 produced to CH_4 converted. In this work, Spagnolo et al. showed interesting results in terms of methane conversion, thermal profiles and energy consumption. Considering the thermal profiles, the presence of an axial temperature profile was found, with minimum temperature values at the outlet end of the reactor below 400 °C due to heat losses by conduction through the power supply terminal.

Calculating the overall energy to produce a certain amount of hydrogen, the heat necessary for the generation of steam was not considered, as was also the case in other bibliographical data [12,15]. The net of heat losses, the energy spent to produce 1 Nm^3 of hydrogen, amounted to approximately 2.78 kWh Nm^{-3} of hydrogen, a value consistent with the data reported in other scientific articles and not far from the energy values required by conventional industrial-scale reformers, as also reported by Atwood and Knight [108]. The electrification of catalysts in steam reforming processes is certainly an interesting solution which, however, sees strong limitations on an industrial scale [12]. If we consider that most of the hydrogen produced by the steam reforming process is used to produce ammonia, it should be noted that about 60% of the ammonia production cost derives from the cost of methane gas used not only as a raw material of the process but also as a fuel.

The important energy contribution given by methane is therefore difficult to replace with electricity. A competitive, low-cost, long-lasting and high-potential electrical energy source is required in order to meet the requirements of the process. However, if one thinks

of an electrified reformer, one should not necessarily think of large industrial scales, but, on the contrary, these reformers lend themselves well to the concept of compact, small and distributed hydrogen modules. Traditional reformers cannot be downsized. Furthermore, another interesting advantage of electrified reformers lies in the maintenance cost: since the material does not have to reach high temperatures on the surface of the tube, it does not undergo severe thermal stress and damage.

Renda et al. studied the electrification of a structured catalyst consisting of a SiC resistance covered with a washcoat based on a silica–mullite composite covered with Ni for the dry and steam reforming reactions. The catalyst was heated by the Joule effect. In this way, it was possible to supply heat to the catalyst directly from the inside, thus reducing the resistance to heat transport. From the data obtained in terms of hydrogen production and energy consumption, it can be seen that, as expected, the energy consumption of the system is strictly linked to the H_2 productivity [10,15]. As also reported by Spagnolo et al. [12], the higher energy consumption was observed at lower space velocity values. This behavior can be explained considering that, with the laboratory scale, the effects of heat dissipation in the reactor have a big role with respect to the low gas flow rate fed to the reactor.

Sekine et al. conducted a catalytic reforming experiment at low temperatures (423 K) [109]. The experimental setup used for this work was a fixed bed reactor connected to two stainless steel bars used as electrodes. In the feed ratio used, S/C was equal to 2, and 200 mg of catalyst was used. Initially, the experiments were conducted to evaluate the effect of an electric field for catalytic reforming on metal catalysts (Pt-, Pd-, Rh-, Ni-) supported on CeO_2. Steam reforming on these catalysts was carried out with and without the electric field, and performed at low temperatures in a range from 423 K to 773 K. It was noted that at low temperature, conventional reforming gave almost zero conversion; subsequently, with the application of the electric field, conversion increased exponentially, especially for the Rh/CeO_2 catalyst. In this study, the authors evaluated the effect of the doping of these catalysts with zirconia in different amounts. It was noted that the conversion of methane increased with the increase of the zirconium content. It was therefore possible to observe that the metal catalysts supported on $Ce_xZr_{1-x}O_2$ are the best among those observed, since they showed a higher activity; in fact, the conversion of methane for electro-reforming increased as the Ce/Zr ratio decreased [109].

It is not always easy and immediate to find data on the energy consumption of these electrified catalytic configurations. Often, since these are applications for heterogeneous catalysts used in endothermic reactions to produce hydrogen, we tend to define the efficiency of the catalyst alone in terms of reagent conversion and product yield, neglecting the aspects linked to the necessary energy consumption and to the homogeneous and lasting heating of the catalyst. Furthermore, the reactor configurations proposed in the literature are very different from each other, and making a comparison is difficult. In this regard, we want to propose a summary table (Table 3) which shows some types of technologies chosen for the electrification of heterogeneous catalysts used in dry and steam methane reforming reactions, in which, in addition to the data relating to the yield and conversion of the reagent, provide information relating to electrical parameters, play and energy consumption. The latter, in particular, are not always available in the literature.

Table 3. Energy consumption among the electrified-structured catalyst proposed in literature for electrified reforming processes and their operating condition.

Process	Heating Element	Catalyst	Electric Parameters	Operating Condition	X_{CH4}; Y_{H2}	Energy Consumption kWh $Nm^{-3}H_2$	Reference
DRM	SiC heating element (Joule Effect)	Ni/Al_2O_3	P = 218 W	CO_2/CH_4 = 1 T = 790 °C.	XCH_4 = 85% YH_2 = 82%	5.1	[15]
SRM	SiC heating element (Joule Effect)	Ni/Al_2O_3	P = 220 W	CH_4/H_2O = 3 T = 790 °C.	XCH_4 = 80% YH_2 = 80%	4.8	[15]
DRM	Stainless electrode (Joule Effect)	Ni/La-ZrO_2	I = 12 mA V = 0.4 kV P = 5 W	T = 576 K CH_4/CO_2 = 1	X_{CH4} 30.2% YH_2 = -	18	[106]
SRM	Stainless electrode rode (Joule Effect)	$Ni/CeZrO_2$ Ce/Zr = 3	I = 3 mA EPC = 1.29 W	T = 190 °C H_2O/CH_4 = 2	X_{CH4} 12% YH_2 = -	3.98	[109]
SRM	Stainless electrode rode (Joule Effect)	$Ni/CeZrO_2$ Ce/Zr = 1	I = 3 mA EPC = 1.53 W			3.21	[109]
SRM	Stainless electrode rode (Joule Effect)	$Ni/CeZrO_2$ Ce/Zr = 0.3	I = 3 mA EPC = 2.54 W			3.75	[109]

3.1. Reactor Configuration for Resistive (Joule) Heating

Considering the current reactor configurations proposed for endothermic processes, they typically include the internal flow of the reactants through a tube configuration in which the heat is supplied from the outside by burning a fossil fuel [110] Therefore, the heating efficiency in these configurations is compromised due to multiple thermal resistances. On the contrary, thinking about the application of resistances for heating the catalysts, they generate heat distributed evenly in the catalyst in direct contact with the fluid. For this purpose, it is interesting to observe which are some of the possible simple reactor configurations that satisfy this requirement. The solutions proposed concern, almost always, schemes of modular reactors with heating by electrical resistance designed for applications in endothermic reactions. The idea of using modular configurations is justified by the energy requirement, and by the difficult scalability of the system thus proposed. In particular, the following two reactor schemes proposed in the literature can be considered, as they represent the configurations more easily applicable even with any changes [105].

3.1.1. Parallel Wire (PW)

In the PW configuration, the reactor is formed by many parallel wires, where each one undergoes the same ΔV as the supply gases flow between the wires.

A schematic unit can be represented as multiple layers of PW, Figure 6, in which each layer of wires can also be located so to reduce the effective hydraulic radius. Such units can be positioned along the flow direction, which is addressed as the "PW module". In a PW module, each unit can be subject to a fixed voltage difference independently, allowing for a customized heating rate and satisfying electrical constraints (e.g., voltage limitation and/or maximum current) [105].

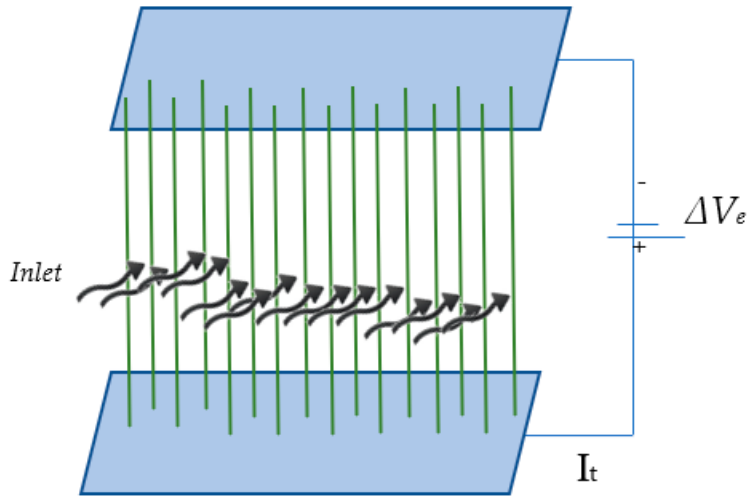

Figure 6. Parallel wires unit reactor configuration. Adapted from [105].

3.1.2. Parallel Tube Reactor (PTR)

This configuration is like the traditional configuration used in endothermic processes (e.g., steam reforming), except that the heating is provided by electricity and by the combustion section. In the PTR, the stacked parallel tubes, each passed through the feed gases, are maintained separate from each other and undergo the same ΔV between inlet and outlet (Figure 7).

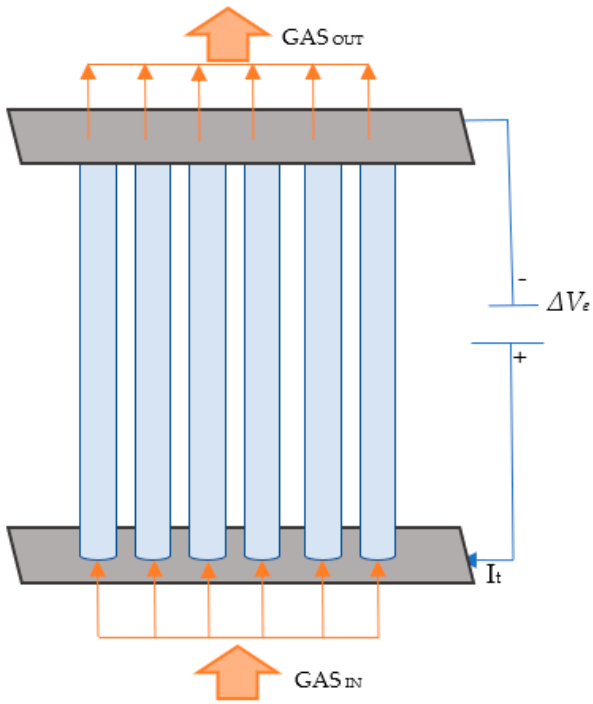

Figure 7. Parallel tube reactor configuration. Adapted from [105].

In this arrangement, the fluid flows internally and has the same direction of the electric current flow. Conversely, in the PW configuration, the fluid flows externally and its direction is perpendicular to the electric current flow. We note that the practical implementation of these reactor configurations can only be achieved if they can be expanded and adapted to the discontinuous nature of renewable energy.

It should be noted that, when covering a wire or tube with a catalytic layer of average thickness between 20–100 μm, the feed gases flow over the electrically heated wires or

tubes where the catalytic reaction and the local composition and temperature are strictly linked. In fact, the temperature of the gas phase next to the floss may cause reforming or other reactions in the gas phase (homogeneous reactions). To identify the materials with the desired catalytic and electrical properties, and to be able to correctly interpret the experimental results in the hypothesis of a scale-up of the process, the understanding of homogeneous–heterogeneous chemistry coupled to local flow conditions and velocity is fundamental. The analysis of this system always requires the characterization of the catalytic properties, in particular of the washcoat, as well as a deep understanding of the transport phenomena [105,111,112].

The factors in terms of both design and operating parameters affecting the conversion of the limiting reactant may be evaluated through small-order models, in which the fluid flow, heat and mass transport are simultaneously coupled in micro–mesoscale. In this sense, different parameters may be considered, including wire properties, the density of catalytic sites, the spacing between wires/tubes, the heating rate, the feed composition, the inlet temperature and the flow rate. For example, in Wismann's work, the evaluation of the functionality of the electrified catalyst was based on a model in which the heat flow was studied on a single heating element consisting of an iron of Fe-Cr-Al characterized by very small temperature gradients [104].

In order to evaluate the possibility that the SiC element, if connected to the electrical grid, can act as heating medium by means of the Joule effect, Renda et al. propose the modeling of the heating element (SiC) and the simulation, which allowed them to evaluate the variation of the electric potential V along the SiC element length and the heat transfer in the solids. The results confirm that, if connected to the electric grid, the SiC element can heat itself by means of the Joule effect, so allowing its use as a support for a catalyst and, consequently, its use in process intensification as a contemporary heating medium and catalyst support [15].

An important and peculiar aspect of these reactor configurations with electrified catalysts is their flexibility and modularity. In fact, it is possible to adjust the number of wires or pipes in the base unit according to the current–voltage and/or power constraints, together with the conversion level to be achieved and the heating requirements. One more important advantage of the modular design of an electrified reactor is that both the shorter start-up and shut-down operations (in the order of magnitude of seconds) may be obtained compared to the several hours or days needed by large traditional fossil fuel reactors. This allows to quickly adapt the number of operating units based on the available power supply [58,105,110].

The idea of electrifying the catalyst, studying in particular the effect of the washcoat, of the interaction between the gas and the electrified catalytic surface, will certainly have further developments, as it is an approach that has interesting characteristics, especially for endothermic reactions.

In fact, with the electrification of the catalyst, heated by the Joule effect, we notice that the heat is generated on the catalytic surface where it is required, thus making the heat transfer much more efficient. Furthermore, the maximum temperature occurs inside the catalytic structure, and no longer in correspondence with the containment walls. This means that the materials of the reactor will also have a greater resistance over time. It is important to underline that, in the proposed configurations, the reactor walls are not subjected to excessively high temperatures, therefore the operating temperature for the reforming processes can be reduced (it is no longer necessary to reach values of 1000 °C to obtain values of 850 °C on the catalyst, and there is no risk of thermal hot spots that can damage the reactor walls). To heat the catalyst, it is possible to use electricity from renewable sources: this saves nonrenewable natural gas, thus reducing CO_2 emissions.

3.2. Remarks

The most interesting aspects of the solutions proposed in the literature for the electrification of reactions for the hydrogen production concern the aspects relating to the transient

time, which, in these cases, is of the order of seconds compared to traditional reactors that take from several hours to a day, and the modularity of the rectors. Perhaps the latter is the most interesting feature of electrified solutions for reforming reactors, already highlighted by some studies in the literature [15,105]. Indeed, it is possible to design the reactor based on the local energy availability of the proposed projects and their modularity, flexibility and ease of scalability. The reactor configurations that provide resistive heating (due to the Joule effect), proposed in various bibliographic studies, can be sized according to the availability of local (renewable) energy. Therefore, a strong interest in this solution emerges from the literature. The researchers carried out their studies both by performing modeling and simulations to understand the behavior of the heat flow along the heating element, and in other cases also trying to validate the data obtained experimentally. The results obtained so far are interesting and certainly need further confirmation and further studies, such as more detailed analyses of flow models, pilot-scale experiments and evaluation of the stability of the catalyst.

4. PEM Fuel Cells

In recent years, many countries and companies have invested heavily in researching and developing new alternative energy sources such as solar, wind, biomass and geothermal energy [113,114]. Hydrogen fuel cells are considered among the most interesting and most suitable energy sources to overcome the problems related to greenhouse gases, climate change and energy shortages [115].

A fuel cell is an electrochemical device capable of directly converting chemical energy into electrical energy through a constant temperature process in which a fuel (typically hydrogen) is combined with oxygen to form water [116].

$$H_2 + \frac{1}{2}O_2 \rightarrow H_2O\ (l) \tag{10}$$

Hydrogen is the most used fuel, but alcohols or gasoline can also be used. Fuel cells are among the most promising systems to produce electrical energy, both for their positive environmental and energy characteristics and for the breadth of possible applications, including distributed generation for power companies, residential and industrial cogeneration, portable generation and traction [116]. A typical fuel cell is made up of three basic elements: an anode, a cathode and an electrolytic membrane (Figure 8). In the cell, hydrogen passes through the anode while oxygen passes through the cathode. In the anode, the hydrogen molecules are split into electrons and protons using a catalyst. Protons pass through the porous membrane of the electrolyte, while electrons are forced through a circuit, thus generating an electric current and heat. On the cathode, protons, electrons and oxygen combine to produce water molecules [117].

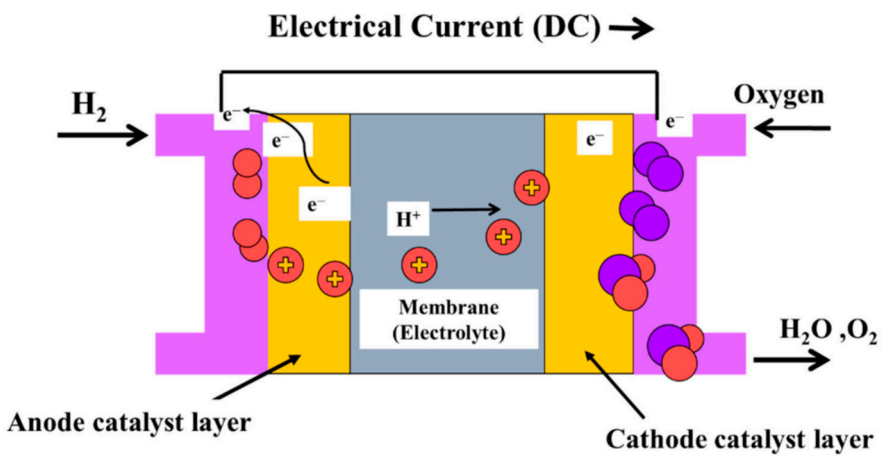

Figure 8. Schematic illustration of fuel cell operation principle. Reprinted from [117].

Fuel cells are receiving considerable attention in scientific research, as they appear to be a very promising alternative for generating clean energy using highly efficient renewable electrolytic hydrogen. Furthermore, fuel cells have the advantage of producing electricity if a fuel source is supplied, thus not needing to be recharged periodically like batteries [117].

4.1. Proton Exchange Membrane Fuel Cells

There are various types of fuel cells which differ in the operating temperature and the type of electrolyte used. Proton exchange membrane fuel cells (PEMFC) are among the most interesting, as they appear to be the most reliable and ready for use in larger scale applications, including the automobile industry and portable devices [118]. In the PEMFCs there is a polymeric electrolytic membrane for the proton conduction. Hydrogen ions, generated by the hydrogen oxidation at the anode, are recombined at the cathode through the polymeric electrolyte membrane with migrating electrons and oxygen, producing water, while electrical energy is generated by electrons in an external circuit connected to a load [119].

The chemical half reactions for the PEMFC are as follows:

Hydrogen Oxidation Reaction (HOR), on the anode [120]:

$$H_2 \rightarrow 2H^+ + 2e^- \tag{11}$$

Oxygen Reduction Reaction (ORR), on the cathode [120]:

$$\frac{1}{2}O_2 + 2H^+ + 2e^- \rightarrow H_2O \tag{12}$$

In PEMFCs (Figure 9), hydrogen, lower alcohols (like methanol and ethanol) and acids (like formic acid) can be used as fuels [121]. However, hydrogen is the most used and recommended since, compared to other usable fuels, its weight-based energy density is the largest and is the easiest to oxidize under the near conditions of room temperature and atmospheric pressure. Furthermore, since oxygen (in air) is used as a comburent, the only products obtainable are electricity, heat and water, thus making it a zero-emission process (greenhouse gas and pollution free) [121]. PEMFCs have significant advantages over other types of fuel cells, including high power densities, low operating temperatures, quick start-up times and easy stacking [118]. In this paragraph, some research progress of platinum-based catalysts and platinum group metal (PGM)-free-based catalysts for PEMFC applications achieved in recent years will be described.

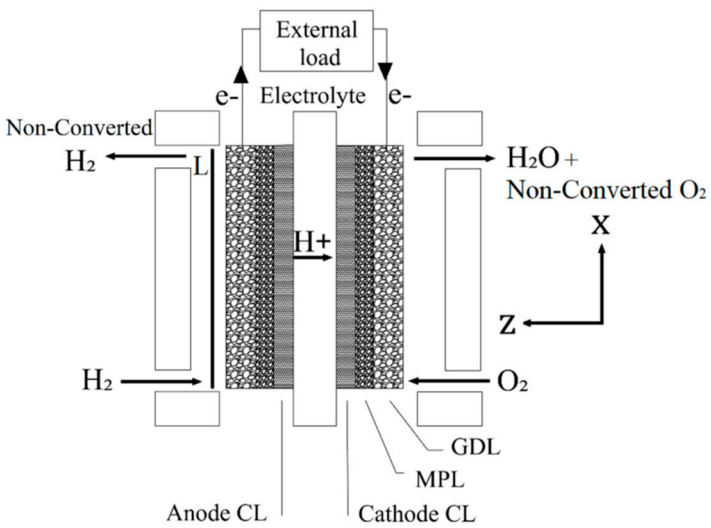

Figure 9. Schematic illustration of PEMFC operation principle. Reprinted from [121].

4.1.1. Pt-Based

Platinum-based catalysts are the choice to realize the optimal adsorption of oxygenate produced in the oxygen reduction reaction (ORR) [122]. Due to the sluggish ORR kinetics at the cathode, and the not particularly high stability of commercial platinum-based catalysts, research is focusing on the development of a catalytic formulations capable of meeting the performance and durability requirements for any applications, and in particular for the automotive one [123]. In this section, the results of some articles focused on the use of platinum-based catalyst in PEMFC applications are briefly argued. A summary table (Table 4) is provided at the end of the section to highlight the results in terms of peak power density (P), mass activity (MA), specific activity (SA) and electrochemical active surface areas (ECSA).

Table 4. Platinum-based catalyst for fuel cells application: Peak power density (P), mass activity (MA), specific activity (SA) and electrochemical active surface areas for selected catalyst for each article (ECSA).

Catalyst	P [W cm_{Pt}^{-2}]	MA [A mg_{Pt}^{-1}]	SA [mA cm_{Pt}^{-2}]	ECSA [m^2 g_{Pt}^{-1}]	Ref
Pt/10wt%SnO_2/C	0.25 (40 °C)	-	-	57	[124]
Pt_3Sc/PECNTs	0.76 (60 °C)	0.0803	-	102.1	[125]
Pt/NbO/CNTs	0.772 (80 °C)	0.057	-	81.62	[126]
$PtSc_{0.5}Ni/MoS_2$@graphene	0.0517 (50 °C)	3.579	4.1	86.27	[127]
Pt-Ni-Ir/C Pt:Ni:Ir = 2:2:1	0.4 (80 °C)	0.0004	-	85	[128]
Pt/VC	0.9 (80 °C)	0.096		56.4	[129]
Pt/rGO	-	-	10.5	0.51	[130]
$Pt/Ti_3O_5Mo_{0.2}Si_{0.4}$	0.97 (80 °C)	-	2.35	89.6	[131]
Pt/CNT-$Ti_3C_2T_x$ (1:1)	0.175 (60 °C)	0.163	0.26	63	[132]
Pt NWs/$Ti_3C_2T_x$-CNT	0.182 (180 °C)	0.32	0.21	63.59	[133]
Pt/TiN–TiO_2	0.392 (70 °C)	-	-	73	[134]
Pt/GCNT	0.38 (160 °C)	-	-	59	[135]
Pt-YO_x/C	-	0.108	0.204	52.82	[136]
Pt_xMg/C	1.275 (80 °C)	1.09	2.67	40	[137]
Au−Pt−Co/C-0.015	-	0.386	0.535	72.2	[138]
Pt-Co/3D rHPGO	-	0.167	0.31	53.1	[139]
Pt/rEGO_2-CB_3	0.537 (60 °C)	0.006416	4.682	41.73	[140]
Pt/CB-$SiO_2$20%,	-	0.26	0.933	29.27	[141]
Pt/CA-200	0.642 (80 °C)	-	-	187.9	[142]
Pt-PBI/MWCNT	0.047 (180 °C)	-	-	43	[143]

Dmitry D. Spasov et al. [124] synthesized a platinum-based catalyst supported on SnO_2-modified carbon for PEMFC applications. The influence of the SnO_2 load, varied between 5% and 40% by weight, was evaluated. The authors demonstrated that the formation of Pt-SnO_2 clusters significantly affects the catalyst structure and performance. The increase of the SnO_2 load promotes the uniformity in the Pt-SnO_2 clusters distribution on the carbon support surface, resulting in improved performance. However, an excessive load of SnO_2 favors particle agglomeration and negatively affects the uniformity of the SnO_2 particle distribution, decreasing the catalyst performance.

Meenakshi Seshadhri Garapati et al. [125] tested a new cathode catalyst for single-cell measurements of PEMFCs, consisting of partially exfoliated carbon nanotubes (PECNTs) on which nanoparticles of the Pt_3Sc alloy have been deposited as an active phase. This catalyst has shown very interesting performances, both in terms of ORR activity and durability, above all thanks to the Pt_3Sc alloy nanoparticles which, due to the excellent interaction with the partially exfoliated carbon nanotubes, allow adsorbing the oxygen molecules with a lower binding energy than Pt.

Reza Alipour MoghadamEsfahani et al. [126] tested a platinum-based catalyst on a NbO combined with multiwalled carbon nanotubes support. The obtained catalyst showed interesting performances for PEMFC applications, as the presence of NbO improved the metal–support interactions and gave the catalyst a high resistance to corrosion.

Padmini Basumatary et al. [127] have developed, for a PEMFCs application, a new catalyst supported by three-dimensional nanoflower-like structures of MoS_2 deposited on graphene sheets, while PtScNi nanoparticles have been grafted on the support as active phases. They also studied the effect of the different doping ratios of Sc, which had a positive effect on the electrocatalytic properties, increasing the activity surface area and the density of the active sites, thus favoring the ensemble effect and the interactions between the nanoparticles of the active phases and the support.

Rui Lin et al. [128] evaluated the performance of a Pt-Ni-Ir ternary alloy used as the active phase of a C-based catalyst for PEMFC applications. The catalyst achieved good performance, both in terms of activity and durability, as the combined presence of Ni and Ir increases the active surface area and improves the uniformity of the Pt distribution.

Fengjuan Zhu et al. [129] reported a synthesis strategy for the realization of a Pt/C-based catalyst, in which citric acid and acetic acid solutions were used to allow pH regulation and facilitate the Pt NPs distribution and the metal active sites generation. Thanks to the synergic effect of these two acids, a catalyst with a high Pt content and a fine and uniform Pt NPs distribution was obtained. The authors believe that these factors have allowed a decrease in the local oxygen transport resistance of the catalyst, thereby providing attractive performance for PEMFC applications.

Jemin Kim et al. [130] carried out a study on the catalytic performance of oxygen reduction catalysts for PEMFCs. Platinum nanoparticles were synthesized on graphene oxide in three reduction states: unreduced, partially reduced and reduced. The results showed that a low concentration of oxygen containing functional group can positively affect the ORR, improving the performance of the catalyst both in terms of activity and durability. Therefore, the catalyst supported by reduced graphene oxide showed the best performance, as it had the lowest concentration of oxygen containing functional group among the tested catalysts.

Reza Alipour Moghadam Esfahani et al. [131] tested the durability of a platinum-based catalyst supported on dual-doped titanium suboxide $Ti_3O_5Mo_{0.2}Si_{0.4}$ for PEMFC applications. This catalyst showed considerable durability during the performed tests due to the ability of the support to stabilize the platinum nanoparticles, thus increasing the resistance to nanoparticles segregation and, consequently, increasing the resistance to deactivation. Furthermore, the presence of Si as a dopant improved both the conductivity of the support and its resistance to corrosion.

Chenxi Xu et al. [132] reported the use of a hybrid material MXene ($Ti_3C_2T_x$)–carbon nanotube (CNT) used as a support for a Pt NPs-based catalyst in PEMFC applications. This hybrid support was prepared by self-assembly of negatively charged $Ti_3C_2T_x$ flakes and positively charged CNTs. This catalyst showed superior performance compared to a commercial Pt/C catalyst, mainly due to the synergic effect of the hybrid support materials.

Ranran Wang et al. [133] evaluated the performance of a catalyst for HT-PEMFC applications consisting of Pt nanowires loaded on a $Ti_3C_2T_x$–CNT hybrid support. With the same support, the Pt nanowire-based catalyst showed superior performance compared to the Pt nanoparticle-based catalyst, both in terms of ORR activity and thermal stability, thanks to the better Pt nanowires electron transport capacity.

Lai Wei et al. [134] evaluated the performance of a Pt-based catalyst in which a TiN-TiO_2 hybrid material was used as a support. This material was obtained starting from TiN treated with alkali to transform a part of it into TiO_2 in order to combine the TiN high conductivity and the TiO_2 high corrosion resistance. Thanks to the combined effect of the two materials and the highly specific surface area of the hybrid support, this catalyst achieved superior performance compared to a commercial Pt/C catalyst, both in terms of ORR activity and stability, making it an interesting catalyst for PEMFCs application.

Yilser Devrim et al. [135] studied the effect of graphitization on multiwalled carbon nanotubes used as a catalytic support in PEMFCs. The carbon nanotubes graphitization assured an improved durability to the final catalyst, enhancing the interactions between the platinum nanoparticles and the support, and thus making the catalyst more resistant to particle sintering.

Tiankuo Chu et al. [136] investigated the influence of yttrium oxides on Pt/C catalysts for PEMFC applications. The yttrium oxides can be easily adsorbed on the Pt crystal surface, thus allowing an increase in the ORR activity and limiting the Pt nanoparticles agglomeration.

Emmanuel Batsa Tetteh et al. [137] studied the performance for PEMFC applications of a carbon-based catalyst in which a platinum–magnesium alloy was used as an active species. This catalyst showed very good catalytic performances, mainly due to the high charges transfer that occurs from Mg to Pt due to the large difference in electronegativity between the two metals. This phenomenon allows the Pt to remain constantly in an electrons-rich state, minimizing its oxidation.

Feng Wang et al. [138] evaluated the performance of an Au-doped Pt-Co/C catalyst for PEMFC applications. The presence of Au allows to obtain a catalyst with a high Pt load already at lower temperatures (≈150 °C) than the typical heat treatments adopted. Furthermore, Au plays a key role in preventing the metal elements leaching during the process. These factors have allowed the catalyst to achieve superior performance, both in terms of ORR activity and stability, compared to a commercial Pt/C catalyst.

Rui Lin et al. [139] used a honeycombed graphene 3D hierarchical porous structure (3D HPG) as a support for a Pt-Co NPs-based catalyst for PEMFC applications. The support was modified with an addition of oxygen groups to allow a better Pt-Co NPs dispersion. The presence of the honeycomb structure protects the Pt-Co NPs from the direct impact of the electrolyte on the catalytic interface, while the presence of the oxygen groups limits the Pt-Co NPs agglomeration, with consequent improved performance compared to a commercial Pt/C catalyst, both in terms of ORR activity and durability.

Zhahoqi Ji et al. [140] have prepared a new hybrid material to be used as a support for platinum-based catalysts in hydrogen fuel cells by combining, in different ratios, reduced electrochemically exfoliated graphene oxide (rEGO) with carbon black (CB). This catalyst, especially in the case of the ratio rEGO:CB = 2:3, showed excellent catalytic performance: the presence of functional groups -NH_2 and graphitic N improved the ORR activity while the structure of the hybrid support hindered the catalyst agglomeration and coarsening.

Jahowa Islam et al. [141] studied the effect of silica coating on the carbon black support in Pt/C-based catalysts for PEMFC applications. The silica-coated carbon-supported catalyst showed better durability than a commercial Pt/C catalyst, as the presence of the silica layer allowed to block the contact between the carbon and the oxygen species, improving catalyst corrosion resistance, and to mitigate the direct contact between Pt and carbon, improving catalyst metal dissolution resistance.

Kevin Gu et al. [142] have developed a Pt-based catalyst supported by a porosity-tunable carbon aerogel (CA) as an alternative to the carbon black (CB) support. Due to the high accessibility of its pores and its higher BET surface area and ECSA compared to the CB-based catalyst, the CA-based catalyst has shown very interesting performance for PEMFC applications.

Enis Oguzhan Eren et al. [143] prepared a platinum-based catalyst using polybenzimidazole (PBI) wrapped carbon nanotubes (MWCNTs) as a support and tested it for possible applications in high-temperature PEMFCs. From the tests carried out, the catalyst proves to be very interesting, especially from the durability point of view. However, the performance of this catalyst in the fuel cell is lower than the commercial Pt/C catalyst, probably due to the polybenzimidazole film over the nanotubes, which can make some of the framework's catalytic areas inaccessible during the single-cell operations.

4.1.2. PGM-Free-Based

Given the high cost and scarcity of Pt, the U.S. Department of Energy (DOE) 2020 target for the total PGM loading in PEMFCs is 0.125 mg_{Pt} cm^{-2}, including 0.025 mg_{Pt} cm^{-2} at the anode and 0.100 mg_{Pt} cm^{-2} at the cathode [144]. Therefore, the significant reduction of Pt appears to be a determining factor for the development of fuel cells. Over the years, significant investments have been made into the research and development of Platinum Group Metal (PGM)-free catalysts for the proton exchange membrane fuel cells in order to enable the first deployment of commercial products [145]. In this section, the results of some articles focused on the use of PGM-free-based catalysts in PEMFC applications are briefly argued. A summary table (Table 5) is provided at the end of the section to highlight the results in terms of peak power density (P), mass activity (MA), specific activity (SA) and electrochemical active surface areas (ECSA).

Table 5. PGM-free-based catalyst for fuel cells application: Peak power density (P), mass activity (MA), specific activity (SA) and electrochemical active surface areas for selected catalyst for each article.

Catalyst	P [W cm^{-2}]	MA [A mg^{-1}]	SA [mA cm^{-2}]	ECSA [m^2 g^{-1}]	Ref
MgO@Phen-Fe-800-3/1	0.63 (70 °C)	-	-	-	[146]
TPI@Z8(SiO_2)-650-C	1.18 (80 °C)	-	-	-	[147]
1.5Fe-ZIF	0.67 (80 °C)	-	-	556	[148]
FeN_4/HOPC-c-1000	0.69 (80 °C)	-	-	-	[149]
Co–N–C@F127	0.87 (80 °C)	-	-	-	[150]
CrN@H-Cr-Nx-C	0.533 (80 °C)	-	-	-	[151]
Co/N/C	0.64 (80 °C)	-	-	-	[152]
Co–N–PCNF	0.71 (80 °C)	-	-	-	[153]
P(AA–AM)(5-1)/Co/N/C	0.66 (80 °C)	-	-	-	[154]
Mn-N-C-HCl-800/1100	0.6 (80 °C)	-	-	-	[155]
Sn/N/C	-	0.0009	-	-	[156]
SiO_2-Fe/N/C	>0.3 (80 °C)	-	-	-	[157]
Fe/N/C 100 nm; I/C = 0.6	0.610 (94 °C)	0.001	-	-	[158]
FeNC-1:30 Ferrocene:ZIF-8 = 1/30	0.602 (70 °C)	-	-	-	[159]
Fe/N/C-300	1.08 (80 °C)	-	-	-	[160]
Fe SAC-MOF-5	0.84 (80 °C)	-	-	-	[161]
0.14Co0.01Fe–CB	0.465 (80 °C)	-	-	-	[162]
FeSa/HP	0.266 (240 °C)	-	-	-	[163]
$IrRu_2$/C	-	-	7.69	-	[164]
Ce SAS/HPNC	0.525 (80 °C)	-	-	-	[165]

Yunfeng Zhan et al. [146] synthesized an Fe/N/C catalyst in which an MgO template was used to favor the FeN_x active sites generation and avoid the Fe/Fe_3C species formation and the metallic Fe agglomeration. The obtained catalyst showed good ORR activity and stability thanks to the FeN_x active sites' higher density and to the improved mass transport properties due to the catalyst mesoporous structures.

Xin Wan et al. [147] synthesized a concave-shaped Fe/N/C single atom catalyst (TPI@Z8(SiO_2)-650-C) and tested it for PEMFC applications. The presence of densely dispersed Fe-N_4 moieties, and the large external surface area, have provided the catalyst with a high density of active sites and, consequently, a high ORR activity.

Hanguang Zhang et al. [148] prepared an N-C-based catalyst doped with Fe in zeolitic imidazolate framework (ZIF)-8 precursors for PEMFC applications. This catalyst showed respectable ORR activity, mainly due to the high density of FeN_4 species in the catalyst. The amount of Fe plays a fundamental role in obtaining a high density of the FeN_4 species, as the authors found that too low an Fe amount in the precursors results in an insufficient

density of FeN_4 sites, while too high an Fe amount leads to the formation of inactive clusters and a consequent significant loss of activity.

Mengfei Qiao et al. [149] prepared and tested, for PEMFC applications, an FeN_4-based catalyst starting from single Fe-doped ZIF-8 crystals carbonized to obtain a hierarchically ordered porous carbon skeleton. The annealing temperature and the Fe doping content were also optimized. The FeN_4/HOPC-c-1000 catalyst (annealing temperature of 1000 °C) achieved good results in terms of activity and durability thanks to its ordered porous structure. Furthermore, annealing temperatures above 800 °C can also enhance the fuel cell performance thanks to an improved chemical stability and electron conductivity.

Yangua He et al. [150] have developed, for PEMFC applications, a new carbon-based catalyst doped with CoN_4, using the synergistic action of a surfactant (Pluronic F127) and ZIF-8 nanocrystals, in order to obtain a higher density of atomically dispersed CoN_4 sites on a core–shell structure. The higher density of the CoN_4 active sites, and the ability of the carbon shell to effectively retain the dominant micropores and to prevent the agglomeration of the single atomic Co sites, are among the main reasons of the good performance obtained by this catalyst.

Hui Yang et al. [151] developed a catalyst in which chromium nitride nanoparticles have been synthesized by the pyrolysis of a ZIF-8@chromium–tannic acid and encapsulated into hollow chromium–nitrogen–carbon capsules. This catalyst (CrN@H-Cr-N_x-C) provided good performance in PEMFC applications, both in terms of activity and stability, thanks to the synergistic effect of the CrN nanoparticles and the CrN_x active sites.

Xiaohong Xie et al. [152] tested the single-atom Co/N/C catalyst for PEMFC applications. The tests have shown a high ORR activity, mainly due to the excellent dispersion of the atomic Co, and a very good durability, due to the promising resistance towards demetallation shown by this catalyst.

Xiaohong Xie et al. [153] have developed, for PEMFC applications, an innovative Co-based M/N/C catalyst whose structure is made up of interconnected porous carbon nanofiber networks with hierarchical structures. The catalyst was prepared by the electrospinning technique with Co-doped ZIFs and dual carrying polymers. The presence of extra graphitic N dopants surrounding the CoN_4 moieties, and the high graphitization of the carbon matrix, are the main reasons for the good performance of this catalyst, both in terms of activity and durability.

Zhengpei Miao et al. [154] used a double crosslinking (DC) hydrogel technique for the preparation of a Co-N-C catalyst, for PEMFC applications, obtained starting from a copolymer of acrylic acid (AA) and acrylamide (AM) coordinated with Co^{2+}. This catalyst has a high CoN_x and doped nitrogen sites density, and a large surface area, thanks to which it has provided good performances in terms of ORR activity. Moreover, the used preparation technique allowed the Co^{2+} metal to strongly stabilize within the reticular structure, thus avoiding the metals Co agglomeration and consequently ensuring a high catalyst stability.

Mengjie Chen et al. [155] prepared a Mn/N/C catalyst by an aqueous solution synthesis and an acid-assisted step-pyrolysis technique. With this preparation technique, a catalyst with very promising performances for PEMFC applications has been synthesized, mainly due to the high catalyst surface area and high graphitic carbon corrosion resistance.

Fang Luo et al. [156] evaluated the performance of a p-block Sn-based M/N/C catalyst for applications in PEMFCs. The catalyst showed good performance, in terms of activity and selectivity, for the ORR reaction, mainly due to the presence of stannic Sn(iv)N_x single metal sites and pyridinic N-combined Sn atoms, which are the catalytically active sites.

Xiaohua Yang et al. [157] investigated the effect of SiO_2 on the performance of a Fe/N/C catalyst in PEMFCs applications. The presence of SiO_2 significantly enhanced the amount of pyridinic-N and defects in the carbon matrix, thus increasing the ORR activity. Furthermore, the properties of mass transport were also improved, as the presence of SiO_2 increased the mesopores of the catalyst and gave the surface greater hydrophobia.

Aman Uddin et al. [158] investigated the performance of an Fe-N-C-based catalyst, in which the Fe particle size and ionomer content were optimized in order to prepare a high-power density cathode for PEFMC applications. The authors found that Fe particle size plays a critical role for fuel cells performance. If the particles are too small, too narrow pores are obtained which do not allow adequate ionomer infiltration, while, if the particles are too large, tortuous paths of the ionomer around the particles are formed, thus causing higher internal resistance to the proton conduction in the catalytic micropores. The results obtained by this catalyst are very promising; however, the degradation rate of the assembled cathode is still high, and further developments are required.

Jinchang Xu et al. [159] synthesized a Fe/N/C catalyst, by means of a two-step pyrolysis technique, to be used in PEMFCs. Ferrocene was used as a Fe precursor while ZIF-8 was used as a carbon source. Through this procedure, the obtained catalyst has a homogeneous distribution of Fe, N and C, and a high specific area which, combined with the high active site content, allowed it to provide good performance in ORR activity.

Shiyang Liu et al. [160] synthesized a Fe-N-C catalyst, for PEMFC applications, exploiting the combined action of the FeN_x active sites and Fe NPs. The catalyst was prepared by Fe-doped carbonized ZIF-8, optimizing the doped Fe loading. According to the authors, the strong interaction between the FeN_x active sites and Fe NPs favors the adsorption/desorption of the ORR products and intermediates; furthermore, Fe NPs allows greater exposure of the usually inaccessible FeN_x active sites, thus improving mass transport. Thanks to these factors, the catalyst showed excellent performance in terms of ORR activity and good stability.

Xiaoying Xie et al. [161] evaluated the performance of a carbon-supported Fe-based catalyst in which the metal organic framework MOF-5 (Zn_4O(1,4-benzenedicarboxylate)$_3$) was used as a precursor for the preparation of a highly porous carbonaceous support. The carbon derived from MOF-5 has a high specific surface area and external surface area, thanks to which it was possible to increase the FeN_x active sites density and provide very interesting performances for PEMFC applications.

Weikang Zhu et al. [162] synthesized a carbon black-supported Co-Fe nanoalloy catalyst obtained by a CoFe-ZIF precursor optimization. A catalyst with highly dispersed and highly active CoFe sites was thus obtained and, thanks to the synergic effect of the Co-Fe alloy nanoparticles and the CoFe-N_x active sites, good performances were achieved in PEMFC applications.

Yi Cheng et al. [163] tested, for high-temperature PEMFC applications, an iron single-atom-based catalyst supported by a carbon nanotube in which hemin porcine (HP, $C_{34}H_{32}ClFeN_4O_4$) was used as iron precursor. The high density of the iron active sites and the high conductivity of the carbon nanotubes have led to promising results in terms of ORR activity. Furthermore, this catalyst showed good stability during tests, as it has a good tolerance to phosphoric acid poisoning.

Seung Woo Lee et al. [164] have prepared, for possible PEMFC applications, a carbon-based catalyst in which an Ir-Ru alloy has been used as the active species. This catalyst has shown superior performance compared to the commercial Pt/C catalyst, as the strong interaction between Ir and Ru improves the HOR activity. The durability of this catalyst was also superior, as the Ir-Ru alloy can suppress the ORR kinetics, thus protecting the cathode catalytic layer.

Mengzhao Zhu et al. [165] synthesized an M/N/C catalyst for PEMFC applications in which Ce single atom sites (SAS) have been incorporated into a hierarchically porous N-doped carbon (HPNC). This catalyst has provided very interesting performances in the ORR activity, thanks to its 3D hierarchically ordered porous architecture, which has improved mass transport and the amount of exposed active sites.

4.1.3. Remarks

With the continuous depletion of the most used energy sources, such as oil and coal, and the worsening of the climatic problems due to their use, reliance on alternative energy

sources that are renewable and that do not negatively affect the surrounding environment is increasingly fundamental. For this purpose, proton exchange membrane fuel cells are one of the most promising technologies for energy production, as they can convert renewable chemical energy into electrical energy with high theoretical efficiency and power density in an environmentally friendly way. However, platinum-based catalysts commercially available still exhibit evident performance and durability problems. Furthermore, the high cost and scarcity of platinum has led the U.S. Department of Energy (DOE) to impose limits on the platinum amount that can be used for fuel cells application. For this purpose, the research is focused on two possible ways to solve these problems:

- The first is to improve the platinum-based catalyst performance by mainly acting on the catalytic formulation using Pt-M alloys or by acting on the catalyst support. The studies have shown that high electrochemical active surface areas and strong interactions between platinum nanoparticles with the catalytic support and/or a second metal can enhance ORR performance, improving, at the same time, the catalyst durability.
- The second is to eliminate the platinum dependence using PGM-free-based catalysts. Although great strides have been made in this field, thanks to very promising metals such as Fe and Co, these catalysts are still not able to meet the required performance and durability standards. However, the studies performed on this type of catalyst have led to very interesting results, making their use very promising for PEMFC applications.

5. Conclusions

The last century has clearly demonstrated the impact of technology on society. The development and use of alternative technologies are mandatory for the transition towards more sustainable industrial processes, aiming at limiting their environmental issues. In fact, the industrial sector, in this challenge towards sustainability, is considering the necessity to fulfil both the peculiar (for example, performance and quality requirements) surrounding (for example, health, safety and environmental risks) requirements of the processes. In fact, the huge contribution of the industry to environmental damages (pollution, climate change, biodiversity loss and resource scarcity) is a reality. In this review the attention has been focused on heating transformation processes, since they are present in any industrial process, impacting the environment with different negative effects, including the consumption of energy and water, or waste generation (including greenhouse gas emissions). In any case, these processes are fundamental for obtaining the transformation of raw materials into the desired products or intermediates that give them added value. In this sense, the generation of energy through electrification is a very promising approach for obtaining more environmentally friendly industrial processes with lower CO_2 emissions compared to conventional technologies in which fossil fuels are employed. Among the others, the reforming processes for producing hydrogen (the clean energy vector of the future) are widely studied for being intensified by electrification. Both resistive/Joule and MW heating may result in an effective enhancement of the performance of catalytic reactors for methane reforming, since they result in the direct heating of the catalyst. So, the increased reaction rate and product selectivity may be obtained. Moreover, smart and compact reactors may be designed and used with a decreased impact on the environment.

6. Outlook

In this context, further efforts are needed for a wide industrialization of the electrified reactors, mainly for the MW-assisted ones. In fact, the scientific community is focused on solving some main issues in which these reactors are still involved. Among the others, (i) methods for the accurate measurement of temperature must be still optimized, and (ii) a deep understanding and knowledge of the hot spot formation due to variation of electromagnetic properties with temperature is mandatory. These issues may be solved by coupling experimental tests and simulation software, which could provide the required

information for low-cost process intensification, but the modeling tools must be further optimized, too, in order to give more precise predictions of the electrified catalytic systems.

Among fuel cells, proton exchange membrane fuel cells can be considered a mature technology for large-scale applications, including for the automotive industry and portable devices. However, further efforts are needed to design efficient and low-cost catalytic systems.

The integration of the different reviewed systems in the way, for example, of a distributed hydrogen production is possible, but only if some main engineering challenges are solved. In fact, (i) the integration of the electrified methane reforming unit with the PEMFC to maximize the energy efficiency may be obtained only if H_2 is effectively separated from the stream exiting the electrified reactor (for example, by using a water–gas shift stage after the reaction step, or a membrane for the H_2 separation) in order to feed high-purity hydrogen, and (ii) more robust and high performing catalysts with a long lifetime are necessary.

Thus, as an important contribution to a sustainable future, the industry and its products can be adapted to a circular economy—a system aimed at eliminating waste, circulating and recycling products, and saving resources and the environment.

Author Contributions: Conceptualization, E.M., M.M., G.I., C.R., S.R., G.F. and V.P.; methodology, E.M., M.M., G.I., C.R., S.R., G.F. and V.P.; software, E.M., M.M., G.I., C.R., S.R., G.F. and V.P.; validation, E.M., M.M., G.I., C.R., S.R., G.F. and V.P.; formal analysis, E.M., M.M., G.I., C.R., S.R., G.F. and V.P.; investigation, E.M., M.M., G.I., C.R., S.R., G.F. and V.P.; resources, E.M., M.M., G.I., C.R., S.R., G.F. and V.P.; data curation, E.M., M.M., G.I., C.R., S.R., G.F. and V.P.; writing—original draft preparation, E.M., M.M., G.I., C.R., S.R., G.F. and V.P.; writing—review and editing, E.M., M.M., G.I., C.R., S.R., G.F. and V.P.; visualization, E.M., M.M., G.I., C.R., S.R., G.F. and V.P.; supervision, E.M., M.M., G.I., C.R., S.R., G.F. and V.P.; project administration, E.M., M.M., G.I., C.R., S.R., G.F. and V.P. All authors have read and agreed to the published version of the manuscript.

Funding: This research was funded by PRIN (Progetti di ricerca di Rilevante Interesse Nazionale)—Bando 2020 Prot. 2020N38E75 "Process for Low-carbon blUe & green hydrogen Generation via Intensified electrified reforming of Natural gas/biogas (PLUG-IN)".

Institutional Review Board Statement: Not applicable.

Informed Consent Statement: Not applicable.

Data Availability Statement: Not applicable.

Acknowledgments: The authors would like to thank PRIN (Progetti di ricerca di Rilevante Interesse Nazionale)—Bando 2020 Prot. 2020N38E75 "Process for Low-carbon blUe & green hydrogen Generation via Intensified electrified reforming of Natural gas/biogas (PLUG-IN)".

Conflicts of Interest: The authors declare no conflict of interest.

Nomenclature

CA	Carbon aerogel
CB	Carbon black
CE	Conversion efficiency
DC	Direct current
DOE	Department of Energy
DRM	Dry reforming of methane
E_{in}	Electrical energy input to the catalyst in kW
ECSA	Electrochemical active surface areas

ER	Electrical energy
F_M	Inlet methane flow in mL min^{-1}
HOPC	Hierarchically ordered porous carbon
HOR	Hydrogen oxidation reaction
HPNC	Hierarchically porous N-doped carbon
MA	Mass activity
MOF	Metal organic framework
MW	Microwave
N	Molar ratio of H_2 produced to CH_4 converted
ORR	Oxygen reduction reaction
P	Peak power density
PECNTs	Partially exfoliated carbon nanotubes
PEMFCs	Proton Exchange Membrane Fuel Cells
PGM	Platinum group metal
POM	Partial oxidation of methane
PTR	Parallel tube reactor
PW	Parallel wire
rEGO	Reduced electrochemically exfoliated graphene oxide
SA	Surface activity
SAS	Single atom sites
SiC	Silicon carbide
SRM	Steam reforming of methane
ZIF	Zeolitic imidazolate framework

References

1. Stankiewicz, A.I.; Nigar, H. Beyond electrolysis: Old challenges and new concepts of electricity-driven chemical reactors. *React. Chem. Eng.* **2020**, *5*, 1005–1016. [CrossRef]
2. Sapountzi, F.; Tsampas, M.; Fredriksson, H.; Gracia, J.; Niemantsverdriet, H. Hydrogen from electrochemical reforming of C1–C3 alcohols using proton conducting membranes. *Int. J. Hydrogen Energy* **2017**, *42*, 10762–10774. [CrossRef]
3. Mahmood, N.; Yao, Y.; Zhang, J.-W.; Pan, L.; Zhang, X.; Zou, J.-J. Electrocatalysts for Hydrogen Evolution in Alkaline Electrolytes: Mechanisms, Challenges, and Prospective Solutions. *Adv. Sci.* **2017**, *5*, 1700464. [CrossRef] [PubMed]
4. Jhong, H.-R.; Ma, S.; Kenis, P.J. Electrochemical conversion of CO_2 to useful chemicals: Current status, remaining challenges, and future opportunities. *Curr. Opin. Chem. Eng.* **2013**, *2*, 191–199. [CrossRef]
5. Sequeira, C.A.C.; Santos, D.M.F. Electrochemical routes for industrial synthesis. *J. Braz. Chem. Soc.* **2009**, *20*, 387–406. [CrossRef]
6. Ding, Q.; Song, B.; Xu, P.; Jin, S. Efficient Electrocatalytic and Photoelectrochemical Hydrogen Generation Using MoS_2 and Related Compounds. *Chem* **2016**, *1*, 699–726. [CrossRef]
7. Iervolino, G.; Tantis, I.; Sygellou, L.; Vaiano, V.; Sannino, D.; Lianos, P. Photocurrent increase by metal modification of Fe_2O_3 photoanodes and its effect on photoelectrocatalytic hydrogen production by degradation of organic substances. *Appl. Surf. Sci.* **2017**, *400*, 176–183. [CrossRef]
8. Iervolino, G.; Vaiano, V.; Rizzo, L. Visible light active Fe-doped TiO_2 for the oxidation of arsenite to arsenate in drinking water. *Chem. Eng. Trans.* **2018**, *70*, 1573–1578.
9. Iervolino, G.; Vaiano, V.; Pepe, G.; Campiglia, P.; Palma, V. Degradation of Acid Orange 7 Azo Dye in Aqueous Solution by a Catalytic-Assisted, Non-Thermal Plasma Process. *Catalysts* **2020**, *10*, 888. [CrossRef]
10. Palma, V.; Cortese, M.; Renda, S.; Ruocco, C.; Martino, M.; Meloni, E. A Review about the Recent Advances in Selected NonThermal Plasma Assisted Solid–Gas Phase Chemical Processes. *Nanomaterials* **2020**, *10*, 1596. [CrossRef]
11. Zhou, D.; Zhou, R.; Zhou, R.; Liu, B.; Zhang, T.; Xian, Y.; Cullen, P.J.; Lu, X.; Ostrikov, K. Sustainable ammonia production by non-thermal plasmas: Status, mechanisms, and opportunities. *Chem. Eng. J.* **2021**, *421*, 129544. [CrossRef]
12. Spagnolo, D.; Cornett, L.; Chuang, K. Direct electro-steam reforming: A novel catalytic approach. *Int. J. Hydrogen Energy* **1992**, *17*, 839–846. [CrossRef]
13. López, E.; Divins, N.J.; Anzola, A.; Schbib, S.; Borio, D.; Llorca, J. Ethanol steam reforming for hydrogen generation over structured catalysts. *Int. J. Hydrogen Energy* **2013**, *38*, 4418–4428. [CrossRef]
14. Ricca, A.; Palma, V.; Martino, M.; Meloni, E. Innovative catalyst design for methane steam reforming intensification. *Fuel* **2017**, *198*, 175–182. [CrossRef]
15. Renda, S.; Cortese, M.; Iervolino, G.; Martino, M.; Meloni, E.; Palma, V. Electrically driven SiC-based structured catalysts for intensified reforming processes. *Catal. Today* **2022**, *383*, 31–43. [CrossRef]
16. Balzarotti, R.; Ambrosetti, M.; Beretta, A.; Groppi, G.; Tronconi, E. Investigation of packed conductive foams as a novel reactor configuration for methane steam reforming. *Chem. Eng. J.* **2019**, *391*, 123494. [CrossRef]
17. Sanz, O.; Velasco, I.; Reyero, I.; Legorburu, I.; Arzamendi, G.; Gandía, L.M.; Montes, M. Effect of the thermal conductivity of metallic monoliths on methanol steam reforming. *Catal. Today* **2016**, *273*, 131–139. [CrossRef]

18. Goyal, H.; Chen, T.-Y.; Chen, W.; Vlachos, D.G. A review of microwave-assisted process intensified multiphase reactors. *Chem. Eng. J.* **2021**, *430*, 133183. [CrossRef]
19. Newman, J.; Bonino, C.A.; Trainham, J.A. The energy future. *Ann. Rev. Chem. Biomol. Eng.* **2018**, *9*, 153–174. [CrossRef]
20. Jones, D.A.; Lelyveld, T.P.; Mavrofidis, S.W.; Kingman, S.W.; Miles, N.J. Microwave heating applications in environmental engineering—A review. *Resour. Conserv. Recycl.* **2001**, *34*, 75–90. [CrossRef]
21. Hu, J.; Wildfire, C.; Stiegman, A.E.; Dagle, R.A.; Shekhawat, D.; Abdelsayed, V.; Bai, X.; Tian, H.; Bogle, M.B.; Hsu, C.; et al. Microwave-driven heterogeneous catalysis for activation of dinitrogen to ammonia under atmospheric pressure. *Chem. Eng. J.* **2020**, *397*, 125388. [CrossRef]
22. Luque, R.; Menendez, J.A.; Arenillas, A.; Cot, J. Microwave-assisted pyrolysis of biomass feedstocks: The way forward? *Energy Environ. Sci.* **2012**, *5*, 5481–5488. [CrossRef]
23. Julian, I.; Ramirez, H.; Hueso, J.L.; Mallada, R.; Santamaria, J. Non-oxidative methane conversion in microwave-assisted structured reactors. *Chem. Eng. J.* **2019**, *377*, 119764. [CrossRef]
24. Zhang, F.; Zhang, X.; Song, Z.; Chen, H.; Zhao, X.; Sun, J.; Mao, Y.; Wang, X.; Wang, W. Fe/HZSM-5 synergizes with biomass pyrolysis carbon to reform CH_4–CO_2 to syngas in microwave field. *Int. J. Hydrogen Energy* **2022**, *47*, 11153–11163. [CrossRef]
25. De Bruyn, M.; Budarin, V.L.; Sturm, G.S.J.; Stefanidis, G.D.; Radoiu, M.; Stankiewicz, A.; Macquarrie, D.J. Subtle Microwave-Induced Overheating Effects in an Industrial Demethylation Reaction and Their Direct Use in the Development of an Innovative Microwave Reactor. *J. Am. Chem. Soc.* **2017**, *139*, 5431–5436. [CrossRef] [PubMed]
26. Horikoshi, S.; Osawa, A.; Sakamoto, S.; Serpone, N. Control of microwave-generated hot spots. Part V. Mechanisms of hot-spot generation and aggregation of catalyst in a microwave-assisted reaction in toluene catalyzed by Pd-loaded AC particulates. *Appl. Catal. A Gen.* **2013**, *460–461*, 52–60. [CrossRef]
27. Musho, T.; Wildfire, C.; Houlihan, N.M.; Sabolsky, E.M.; Shekhawat, D. Study of Cu_2O particle morphology on microwave field enhancement. *Mater. Chem. Phys.* **2018**, *216*, 278–284. [CrossRef]
28. Chen, W.; Gutmann, B.; Kappe, C.O. Characterization of Microwave-Induced Electric Discharge Phenomena in Metal-Solvent Mixtures. *ChemistryOpen* **2012**, *1*, 39–48. [CrossRef]
29. Horikoshi, S.; Osawa, A.; Abe, M.; Serpone, N. On the Generation of Hot-Spots by Microwave Electric and Magnetic Fields and Their Impact on a Microwave-Assisted Heterogeneous Reaction in the Presence of Metallic Pd Nanoparticles on an Activated Carbon Support. *J. Phys. Chem. C* **2011**, *115*, 23030–23035. [CrossRef]
30. Horikoshi, S.; Suttisawat, Y.; Osawa, A.; Takayama, C.; Chen, X.; Yang, S.; Sakai, H.; Abe, M.; Serpone, N. Organic syntheses by microwave selective heating of novel metal/CMC catalysts–The Suzuki-Miyaura coupling reaction in toluene and the dehydrogenation of tetralin in solvent-free media. *J. Catal.* **2012**, *289*, 266–271. [CrossRef]
31. Horikoshi, S.; Osawa, A.; Sakamoto, S.; Serpone, N. Control of microwave generated hot spots. Part IV. Control of hot spots on a heterogeneous microwaveabsorber catalyst surface by a hybrid internal/external heating method. *Chem. Eng. Process. Process Intensif.* **2013**, *69*, 52–56. [CrossRef]
32. Zhang, X.; Hayward, D.O.; Mingos, D.M.P. Apparent equilibrium shifts and hot-spot formation for catalytic reactions induced by microwave dielectric heating. *Chem. Commun.* **1999**, *11*, 975–976. [CrossRef]
33. Horikoshi, S.; Kamata, M.; Mitani, T.; Serpone, N. Control of Microwave-Generated Hot Spots. 6. Generation of Hot Spots in Dispersed Catalyst Particulates and Factors That Affect Catalyzed Organic Syntheses in Heterogeneous Media. *Ind. Eng. Chem. Res.* **2014**, *53*, 14941–14947. [CrossRef]
34. Suttisawat, Y.; Horikoshi, S.; Sakai, H.; Abe, M. Hydrogen production from tetralin over microwave-accelerated Pt-supported activated carbon. *Int. J. Hydrogen Energy* **2010**, *35*, 6179–6183. [CrossRef]
35. Suttisawat, Y.; Horikoshi, S.; Sakai, H.; Rangsunvigit, P.; Abe, M. Enhanced conversion of tetralin dehydrogenation under microwave heating: Effects of temperature variation. *Fuel Process. Technol.* **2011**, *95*, 27–32. [CrossRef]
36. Horikoshi, S.; Kamata, M.; Sumi, T.; Serpone, N. Selective heating of Pd/AC catalyst in heterogeneous systems for the microwave-assisted continuous hydrogen evolution from organic hydrides: Temperature distribution in the fixed-bed reactor. *Int. J. Hydrogen Energy* **2016**, *41*, 12029–12037. [CrossRef]
37. Manno, R.; Sebastian, V.; Mallada, R.; Santamaria, J.S. 110th Anniversary: Nucleation of Ag Nanoparticles in Helical Microfluidic Reactor. Comparison between Microwave and Conventional Heating. *Ind. Eng. Chem. Res.* **2019**, *58*, 12702–12711. [CrossRef]
38. Ramirez, A.; Hueso, J.L.; Abian, M.; Alzueta, M.U.; Mallada, R.; Santamaria, J. Escaping undesired gas-phase chemistry: Microwave-driven selectivity enhancement in heterogeneous catalytic reactors. *Sci. Adv.* **2019**, *5*, eaau9000. [CrossRef]
39. Meloni, E.; Martino, M.; Ricca, A.; Palma, V. Ultracompact methane steam reforming reactor based on microwaves susceptible structured catalysts for distributed hydrogen production. *Int. J. Hydrogen Energy* **2020**, *46*, 13729–13747. [CrossRef]
40. Ramirez, A.; Hueso, J.L.; Mallada, R.; Santamaria, J. In situ temperature measurements in microwave-heated gas-solid catalytic systems. Detection of hot spots and solid-fluid temperature gradients in the ethylene epoxidation reaction. *Chem. Eng. J.* **2017**, *316*, 50–60. [CrossRef]
41. Ramirez, A.; Hueso, J.L.; Mallada, R.; Santamaria, J. Microwave-activated structured reactors to maximize propylene selectivity in the oxidative dehydrogenation of propane. *Chem. Eng. J.* **2020**, *393*, 124746. [CrossRef]
42. Suttisawat, Y.; Sakai, H.; Abe, M.; Rangsunvigit, P.; Horikoshi, S. Microwave effect in the dehydrogenation of tetralin and decalin with a fixed-bed reactor. *Int. J. Hydrogen Energy* **2012**, *37*, 3242–3250. [CrossRef]

43. Haneishi, N.; Tsubaki, S.; Abe, E.; Maitani, M.M.; Suzuki, E.-I.; Fujii, S.; Fukushima, J.; Takizawa, H.; Wada, Y. Enhancement of Fixed-bed Flow Reactions under Microwave Irradiation by Local Heating at the Vicinal Contact Points of Catalyst Particles. *Sci. Rep.* **2019**, *9*, 222. [CrossRef] [PubMed]
44. Durka, T.; Stefanidis, G.D.; Van Gerven, T.; Stankiewicz, A.I. Microwave-activated methanol steam reforming for hydrogen production. *Int. J. Hydrogen Energy* **2011**, *36*, 12843–12852. [CrossRef]
45. Meloni, E.; Martino, M.; Pullumbi, P.; Brandani, F.; Palma, V. Intensification of TSA processes using a microwave-assisted regeneration step. *Chem. Eng. Process. Process Intensif.* **2020**, *160*, 108291. [CrossRef]
46. Ergan, B.T.; Bayramoğlu, M.; Özcan, S. Emulsion polymerization of styrene under continuous microwave irradiation. *Eur. Polym. J.* **2015**, *69*, 374–384. [CrossRef]
47. Ricciardi, L.; Verboom, W.; Lange, J.; Huskens, J. Reactive Extraction Enhanced by Synergic Microwave Heating: Furfural Yield Boost in Biphasic Systems. *ChemSusChem* **2020**, *13*, 3589–3593. [CrossRef]
48. Motasemi, F.; Gerber, A.G. Multicomponent conjugate heat and mass transfer in biomass materials during microwave pyrolysis for biofuel production. *Fuel* **2018**, *211*, 649–660. [CrossRef]
49. Aguilera, A.F.; Tolvanen, P.; Eränen, K.; Wärnå, J.; Leveneur, S.; Marchant, T.; Salmi, T. Kinetic modelling of Prileschajew epoxidation of oleic acid under conventional heating and microwave irradiation. *Chem. Eng. Sci.* **2019**, *199*, 426–438. [CrossRef]
50. Aguilera, A.F.; Tolvanen, P.; Wärnå, J.; Leveneur, S.; Salmi, T. Kinetics and reactor modelling of fatty acid epoxidation in the presence of heterogeneous catalyst. *Chem. Eng. J.* **2019**, *375*, 121936. [CrossRef]
51. Li, H.; Zhao, Z.; Xiouras, C.; Stefanidis, G.D.; Li, X.; Gao, X. Fundamentals and applications of microwave heating to chemicals separation processes. *Renew. Sustain. Energy Rev.* **2019**, *114*, 109316. [CrossRef]
52. Palma, V.; Barba, D.; Cortese, M.; Martino, M.; Renda, S.; Meloni, E. Microwaves and Heterogeneous Catalysis: A Review on Selected Catalytic Processes. *Catalysts* **2020**, *10*, 246. [CrossRef]
53. Enger, B.C.; Lødeng, R.; Holmen, A. A review of catalytic partial oxidation of methane to synthesis gas with emphasis on reaction mechanisms over transition metal catalysts. *Appl. Catal. A Gen.* **2008**, *346*, 1–27. [CrossRef]
54. Fisher, F.; Tropsch, H. Conversion of methane into hydrogen and carbon monoxide. *Brennst.-Chem.* **1928**, *9*, 39–46.
55. Reitmeier, R.E.; Atwood, K.; Bennett, H.; Baugh, H. Production of synthetic gas-reaction of light hydrocarbons with steam and carbon dioxide. *Ind. Eng. Chem.* **1948**, *40*, 620–626. [CrossRef]
56. Lewis, W.K.; Gilliland, E.R.; Reed, W.A. Reaction of methane with copper oxide in a fluidized bed. *Ind. Eng. Chem.* **1949**, *41*, 1227–1237. [CrossRef]
57. Li, F.; Ao, M.; Pham, G.H.; Jin, Y.; Nguyen, M.H.; Alawi, N.M.; Tade, M.O.; Liu, S. A novel UiO-66 encapsulated 12-silicotungstic acid catalyst for dimethyl ether synthesis from syngas. *Catal. Today* **2020**, *355*, 3–9. [CrossRef]
58. de García, I.D.; Stankiewicz, A.; Nigar, H. Syngas production via microwave-assisted dry reforming of methane. *Catal. Today* **2020**, *362*, 72–80. [CrossRef]
59. Pakhare, D.; Spivey, J. A review of dry (CO_2) reforming of methane over noble metal catalysts. *Chem. Soc. Rev.* **2014**, *43*, 7813–7837. [CrossRef]
60. Meloni, E.; Martino, M.; Palma, V. A Short Review on Ni Based Catalysts and Related Engineering Issues for Methane Steam Reforming. *Catalysts* **2020**, *10*, 352. [CrossRef]
61. Etminan, A.; Sadrnezhaad, S.K. A two step Microwave-assisted coke resistant mesoporous Ni-Co catalyst for methane steam reforming. *Fuel* **2022**, *317*, 122411. [CrossRef]
62. Sokolov, S.; Kondratenko, E.V.; Pohl, M.-M.; Barkschat, A.; Rodemerck, U. Stable low-temperature dry reforming of methane over mesoporous La_2O_3-ZrO_2 supported Ni catalyst. *Appl. Catal. B Environ.* **2012**, *113*, 19–30. [CrossRef]
63. Baudouin, D.; Rodemerck, U.; Krumeich, F.; Mallmann, A.D.; Szeto, K.C.; Ménard, H.; Veyre, L.; Candy, J.-P.; Webb, P.B.; Thieuleux, C.; et al. Particle size effect in the low temperature reforming of methane by carbon dioxide on silica-supported Ni nanoparticles. *J. Catal.* **2013**, *297*, 27–34. [CrossRef]
64. Matsumura, Y.; Nakamori, T. Steam reforming of methane over nickel catalysts at low reaction temperature. *Appl. Catal. A Gen.* **2004**, *258*, 107–114. [CrossRef]
65. An, Y.; Dou, J.; Tian, L.; Zhao, X.; Yu, J. Role of microwave during microwave-assisted catalytic reforming of guaiacol, syringolbio-oil as model compounds. *J. Anal. Appl. Pyrolysis* **2021**, *158*, 105290. [CrossRef]
66. Nguyen, H.M.; Sunarso, J.; Li, C.; Pham, G.H.; Phan, C.; Liu, S. Microwave-assisted catalytic methane reforming: A review. *Appl. Catal. A Gen.* **2020**, *599*, 117620. [CrossRef]
67. Díaz-Ortiz, Á.; Prieto, P.; de la Hoz, A. A critical overview on the effect of microwave irradiation in organic synthesis. *Chem. Rec.* **2019**, *19*, 85–97. [CrossRef]
68. Xu, W.; Zhou, J.; Ou, Y.; Luo, Y.; You, Z. Microwave selective effect: A new approach towards oxygen inhibition removal for highly-effective NO decomposition by Microwave catalysis over $BaMn_xMg_{1-x}O_3$ mixed oxides at low temperature under excess oxygen. *Chem. Commun.* **2015**, *51*, 4073–4076. [CrossRef]
69. Xu, W.; Wang, Q.; Peng, K.; Chen, F.; Han, X.; Wang, X.; Zhou, J. Development of $MgCo_2O_4$–$BaCO_3$ composites as microwave catalysts for the highly effective direct decomposition of NO under excess O_2 at a low temperature. *Catal. Sci. Technol.* **2019**, *9*, 4276–4285. [CrossRef]
70. Garcia-Costa, A.L.; Zazo, J.A.; Casas, J.A. Microwave-assisted catalytic wet peroxide oxidation: Energy optimization. *Sep. Purif. Technol.* **2019**, *215*, 62–69. [CrossRef]

71. Nozariasbmarz, A.; Dsouza, K.; Vashaee, D. Field induced decrystallization of silicon: Evidence of a microwave non-thermal effect. *Appl. Phys. Lett.* **2018**, *112*, 093103. [CrossRef]
72. Einaga, H.; Nasu, Y.; Oda, M.; Saito, H. Catalytic performances of perovskite oxides for CO oxidation under microwave irradiation. *Chem. Eng. J.* **2016**, *283*, 97–104. [CrossRef]
73. Stuerga, D.A.C.; Gaillard, P. Microwave Athermal Effects in Chemistry: A Myth's Autopsy: Part II: Orienting effects and thermodynamic consequences of electric field. *J. Microw. Power Electromagn. Energy* **1996**, *31*, 101–113. [CrossRef]
74. Stuerga, D.A.C.; Gaillard, P. Microwave Athermal Effects in Chemistry: A Myth's Autopsy: Part I: Historical background and fundamentals of wave-matter interaction. *J. Microw. Power Electromagn. Energy* **1996**, *31*, 87–100. [CrossRef]
75. Xu, W.; Zhou, J.; Su, Z.; Ou, Y.; You, Z. Microwave catalytic effect: A new exact reason for microwave-driven heterogeneous gas-phase catalytic reactions. *Catal. Sci. Technol.* **2015**, *6*, 698–702. [CrossRef]
76. Bai, X.; Robinson, B.; Killmer, C.; Wang, Y.; Li, L.; Hu, J. Microwave catalytic reactor for upgrading stranded shale gas to aromatics. *Fuel* **2019**, *243*, 485–492. [CrossRef]
77. Hunt, J.; Ferrari, A.; Lita, A.; Crosswhite, M.; Ashley, B.; Stiegman, A.E. Microwave-Specific Enhancement of the Carbon–Carbon Dioxide (Boudouard) Reaction. *J. Phys. Chem. C* **2013**, *117*, 26871–26880. [CrossRef]
78. Bai, X.; Muley, P.D.; Musho, T.; Abdelsayed, V.; Robinson, B.; Caiola, A.; Shekhawat, D.; Jiang, C.; Hu, J. A combined experimental and modeling study of Microwave-assisted methane dehydroaromatization process. *Chem. Eng. J.* **2022**, *433*, 134445. [CrossRef]
79. Goyal, H.; Mehdad, A.; Lobo, R.F.; Stefanidis, G.; Vlachos, D.G. Scaleup of a Single-Mode Microwave Reactor. *Ind. Eng. Chem. Res.* **2019**, *59*, 2516–2523. [CrossRef]
80. Sturm, G.S.J.; Verweij, M.D.; Van Gerven, T.; Stankiewicz, A.I.; Stefanidis, G. On the effect of resonant microwave fields on temperature distribution in time and space. *Int. J. Heat Mass Transf.* **2012**, *55*, 3800–3811. [CrossRef]
81. Chen, T.-Y.; Baker-Fales, M.; Vlachos, D.G. Operation and Optimization of Microwave-Heated Continuous-Flow Microfluidics. *Ind. Eng. Chem. Res.* **2020**, *59*, 10418–10427. [CrossRef]
82. Malhotra, A.; Chen, W.; Goyal, H.; Plaza-Gonzalez, P.J.; Julian, I.; Catala-Civera, J.M.; Vlachos, D.G. Temperature Homogeneity under Selective and Localized Microwave Heating in Structured Flow Reactors. *Ind. Eng. Chem. Res.* **2021**, *60*, 6835–6847. [CrossRef]
83. Robinson, J.; Kingman, S.; Irvine, D.; Licence, P.; Smith, A.; Dimitrakis, G.; Obermayer, D.; Kappe, C.O. Electromagnetic simulations of microwave heating experiments using reaction vessels made out of silicon carbide. *Phys. Chem. Chem. Phys.* **2010**, *12*, 10793–10800. [CrossRef] [PubMed]
84. Sanz-Moral, L.M.; Navarrete, A.; Sturm, G.; Link, G.; Rueda, M.; Stefanidis, G.; Martín, Á. Release of hydrogen from nanoconfined hydrides by application of microwaves. *J. Power Sources* **2017**, *353*, 131–137. [CrossRef]
85. Nigar, H.; Sturm, G.S.J.; Garcia-Baños, B.; Peñaranda-Foix, F.L.; Catalá-Civera, J.M.; Mallada, R.; Stankiewicz, A.; Santamaría, J. Numerical analysis of microwave heating cavity: Combining electromagnetic energy, heat transfer and fluid dynamics for a NaY zeolite fixed-bed. *Appl. Therm. Eng.* **2019**, *155*, 226–238. [CrossRef]
86. Zhang, C.; Liao, L.; Gong, S.S. Recent developments in microwave-assisted polymerization with a focus on ring-opening polymerization. *Green Chem.* **2007**, *9*, 303–314. [CrossRef]
87. Ebner, C.; Bodner, T.; Stelzer, F.; Wiesbrock, F. One Decade of Microwave-Assisted Polymerizations: Quo vadis? *Macromol. Rapid Commun.* **2011**, *32*, 254–288. [CrossRef]
88. Hoogenboom, R.; Schubert, U.S. Microwave-Assisted Polymer Synthesis: Recent Developments in a Rapidly Expanding Field of Research. *Macromol. Rapid Commun.* **2007**, *28*, 368–386. [CrossRef]
89. Van Putten, R.-J.; Van Der Waal, J.C.; De Jong, E.; Rasrendra, C.B.; Heeres, H.J.; De Vries, J.G. Hydroxymethylfurfural, A Versatile Platform Chemical Made from Renewable Resources. *Chem. Rev.* **2013**, *113*, 1499–1597. [CrossRef]
90. Caratzoulas, S.; Davis, M.E.; Gorte, R.J.; Gounder, R.; Lobo, R.F.; Nikolakis, V.; Sandler, S.I.; Snyder, M.A.; Tsapatsis, M.; Vlachos, D.G. Challenges of and Insights into Acid-Catalyzed Transformations of Sugars. *J. Phys. Chem. C* **2014**, *118*, 22815–22833. [CrossRef]
91. Chen, T.-Y.; Cheng, Z.; Desir, P.; Saha, B.; Vlachos, D.G. Fast microflow kinetics and acid catalyst deactivation in glucose conversion to 5-hydroxymethylfurfural. *React. Chem. Eng.* **2020**, *6*, 152–164. [CrossRef]
92. Palma, V.; Martino, M.; Meloni, E.; Ricca, A. Novel structured catalysts configuration for intensification of steam reforming of methane. *Int. J. Hydrogen Energy* **2017**, *42*, 1629–1638. [CrossRef]
93. Bianchi, E.; Heidig, T.; Visconti, C.G.; Groppi, G.; Freund, H.; Tronconi, E. An appraisal of the heat transfer properties of metallic open-cell foams for strongly exo-/endo-thermic catalytic processes in tubular reactors. *Chem. Eng. J.* **2012**, *198–199*, 512–528. [CrossRef]
94. Ramírez, A.; Hueso, J.L.; Mallada, R.; Santamaría, J. Ethylene epoxidation in microwave heated structured reactors. *Catal. Today* **2016**, *273*, 99–105. [CrossRef]
95. Palma, V.; Ricca, A.; Martino, M.; Meloni, E. Innovative structured catalytic systems for methane steam reforming intensification. *Chem. Eng. Process. Process Intensif.* **2017**, *120*, 207–215. [CrossRef]
96. Zhang, H.; Geerlings, H.; Lin, J.; Chin, W.S. Rapid microwave hydrogen release from MgH_2 and other hydrides. *Int. J. Hydrogen Energy* **2011**, *36*, 7580–7586. [CrossRef]
97. Mao, Y.; Yang, S.; Xue, C.; Zhang, M.; Wang, W.; Song, Z.; Zhao, X.; Sun, J. Rapid degradation of malachite green by $CoFe_2O_4$–SiC foam under microwave radiation. *R. Soc. Open Sci.* **2018**, *5*, 180085. [CrossRef]

98. Gangurde, L.S.; Sturm, G.S.J.; Valero-Romero, M.J.; Mallada, R.; Santamaria, J.; Stankiewicza, A.I.; Stefanidis, G.D. Synthesis, characterization, and application of ruthenium-doped $SrTiO_3$ perovskite catalysts for microwave-assisted methane dry reforming. *Chem. Eng. Process. Process Intensif.* **2018**, *127*, 178–190. [CrossRef]
99. Marin, C.M.; Popczun, E.J.; Nguyen-Phan, T.-D.; De Tafen, N.; Alfonso, D.; Waluyo, I.; Hunt, A.; Kauffman, D.R. Designing perovskite catalysts for controlled active-site exsolution in the microwave dry reforming of methane. *Appl. Catal. B Environ.* **2020**, *284*, 119711. [CrossRef]
100. Nguyen, H.M.; Pham, G.H.; Tade, M.; Phan, C.; Vagnoni, R.; Liu, S. Microwave-Assisted Dry and Bi-reforming of Methane over M–Mo/TiO_2 (M = Co, Cu) Bimetallic Catalysts. *Energy Fuels* **2020**, *34*, 7284–7294. [CrossRef]
101. Li, R.; Xu, W.; Deng, J.; Zhou, J. Coke-Resistant Ni−Co/ZrO_2−CaO-Based Microwave Catalyst for Highly Effective Dry Reforming of Methane by Microwave Catalysis. *Ind. Eng. Chem. Res.* **2021**, *60*, 17458–17468. [CrossRef]
102. Sharifvaghefi, S.; Shirani, B.; Eic, M.; Zheng, Y. Application of Microwave in Hydrogen Production from Methane Dry Reforming: Comparison between the Conventional and Microwave-Assisted Catalytic Reforming on Improving the Energy Efficiency. *Catalysts* **2019**, *9*, 618. [CrossRef]
103. Chen, W.; Malhotra, A.; Yu, K.; Zheng, W.; Plaza-Gonzalez, P.J.; Catala-Civera, J.M.; Santamaria, J.; Vlachos, D.G. Intensified microwave-assisted heterogeneous catalytic reactors for sustainable chemical manufacturing. *Chem. Eng. J.* **2021**, *420*, 130476. [CrossRef]
104. Wismann, S.T.; Engbæk, J.S.; Vendelbo, S.B.; Eriksen, W.L.; Frandsen, C.; Mortensen, P.M.; Chorkendorff, I. Electrified Methane Reforming: Understanding the Dynamic Interplay. *Ind. Eng. Chem. Res.* **2019**, *58*, 23380–23388. [CrossRef]
105. Balakotaiah, V.; Ratnakar, R.R. Modular reactors with electrical resistance heating for hydrocarbon cracking and other endothermic reactions. *AIChE J.* **2021**, *68*, e17542. [CrossRef]
106. Yabe, T.; Mitarai, K.; Oshima, K.; Ogo, S.; Sekine, Y. Low-temperature dry reforming of methane to produce syngas in an electric field over La-doped Ni/ZrO_2 catalysts. *Fuel Process. Technol.* **2017**, *158*, 96–103. [CrossRef]
107. Rieks, M.; Bellinghausen, R.; Kockmann, N.; Mleczko, L. Experimental study of methane dry reforming in an electrically heated reactor. *Int. J. Hydrogen Energy* **2015**, *40*, 15940–15951. [CrossRef]
108. Atwood, K.; Knight, C.B. Relbrming kinetics and catalysis. In *Fertilizer Science and Technology*; Slack, A.V., James, G.R., Eds.; Marcel Dekker: New York, NY, USA, 1973; Volume 2.
109. Sekine, Y.; Haraguchi, M.; Matsukata, M.; Kikuchi, E. Low temperature steam reforming of methane over metal catalyst supported on $Ce_xZr_{1-x}O_2$ in an electric field. *Catal. Today* **2011**, *171*, 116–125. [CrossRef]
110. Froment, G.; Bischoff, K.; Wilde, J. Transport Processes with Reactions Catalyzed by Solids. In *Chemical Reactor Analysis and Design*, 2nd ed.; John Wiley & Sons: New York, NY, USA, 1990; pp. 148–149.
111. Ratnakar, R.R.; Dadi, R.K.; Balakotaiah, V. Multi-scale reduced order models for transient simulation of multi-layered monolith reactors. *Chem. Eng. J.* **2018**, *352*, 293–305. [CrossRef]
112. Sarkar, B.; Ratnakar, R.R.; Balakotaiah, V. Multi-scale coarse-grained continuum models for bifurcation and transient analysis of coupled homogeneous-catalytic reactions in monoliths. *Chem. Eng. J.* **2020**, *407*, 126500. [CrossRef]
113. Olabi, A.; Wilberforce, T.; Abdelkareem, M.A. Fuel cell application in the automotive industry and future perspective. *Energy* **2020**, *214*, 118955. [CrossRef]
114. Fan, L.; Tu, Z.; Chan, S.H. Recent development of hydrogen and fuel cell technologies: A review. *Energy Rep.* **2021**, *7*, 8421–8446. [CrossRef]
115. Song, Y.; Zhang, C.; Ling, C.-Y.; Han, M.; Yong, R.-Y.; Sun, D.; Chen, J. Review on current research of materials, fabrication and application for bipolar plate in proton exchange membrane fuel cell. *Int. J. Hydrogen Energy* **2019**, *45*, 29832–29847. [CrossRef]
116. Treccani, Il Portale Del Sapere. Available online: https://www.treccani.it/enciclopedia/celle-a-combustibile_%28Enciclopedia-della-Scienza-e-della-Tecnica%29/ (accessed on 16 December 2021).
117. Alashkar, A.; Al-Othman, A.; Tawalbeh, M.; Qasim, M. A Critical Review on the Use of Ionic Liquids in Proton Exchange Membrane Fuel Cells. *Membranes* **2022**, *12*, 178. [CrossRef] [PubMed]
118. Tzelepis, S.; Kavadias, K.A.; Marnellos, G.E.; Xydis, G. A review study on proton exchange membrane fuel cell electrochemical performance focusing on anode and cathode catalyst layer modelling at macroscopic level. *Renew. Sustain. Energy Rev.* **2021**, *151*, 111543. [CrossRef]
119. Ren, X.; Wang, Y.; Liu, A.; Zhang, Z.; Lv, Q.; Liu, B. Current progress and performance improvement of Pt/C catalysts for fuel cells. *J. Mater. Chem. A* **2020**, *8*, 24284–24306. [CrossRef]
120. Manoharan, Y.; Hosseini, S.E.; Butler, B.; Alzhahrani, H.; Senior, B.T.F.; Ashuri, T.; Krohn, J. Hydrogen Fuel Cell Vehicles; Current Status and Future Prospect. *Appl. Sci.* **2019**, *9*, 2296. [CrossRef]
121. Pourrahmani, H.; Shakeri, H.; Van Herle, J. Thermoelectric Generator as the Waste Heat Recovery Unit of Proton Exchange Membrane Fuel Cell: A Numerical Study. *Energies* **2022**, *15*, 3018. [CrossRef]
122. Huang, L.; Zaman, S.; Tian, X.; Wang, Z.; Fang, W.; Xia, B.Y. Advanced Platinum-Based Oxygen Reduction Electrocatalysts for Fuel Cells. *Accounts Chem. Res.* **2021**, *54*, 311–322. [CrossRef]
123. Wang, X.X.; Swihart, M.T.; Wu, G. Achievements, challenges and perspectives on cathode catalysts in proton exchange membrane fuel cells for transportation. *Nat. Catal.* **2019**, *2*, 578–589. [CrossRef]

124. Spasov, D.D.; Ivanova, N.A.; Pushkarev, A.S.; Pushkareva, I.V.; Presnyakova, N.N.; Chumakov, R.G.; Presnyakov, M.Y.; Grigoriev, S.A.; Fateev, V.N. On the Influence of Composition and Structure of Carbon-Supported Pt-SnO_2 Hetero-Clusters onto Their Electrocatalytic Activity and Durability in PEMFC. *Catalysts* **2019**, *9*, 803. [CrossRef]
125. Garapati, M.S.; Sundara, R. Highly efficient and ORR active platinum-scandium alloy-partially exfoliated carbon nanotubes electrocatalyst for Proton Exchange Membrane Fuel Cell. *Int. J. Hydrogen Energy* **2019**, *44*, 10951–10963. [CrossRef]
126. MoghadamEsfahani, R.A.; Vankova, S.K.; Easton, E.B.; Ebralidze, I.; Specchia, S. A hybrid Pt/NbO/CNTs catalyst with high activity and durability for oxygen reduction reaction in PEMFC. *Renew. Energy* **2020**, *154*, 913–924. [CrossRef]
127. Basumatarya, P.; Konwarb, D.; Yoon, Y.S. Conductivity-tailored PtNi/MoS_2 3D nanoflower catalyst via Sc doping as a hybrid anode for a variety of hydrocarbon fuels in proton exchange membrane fuel cells. *Appl. Catal. B Environ.* **2020**, *267*, 118724. [CrossRef]
128. Lin, R.; Che, L.; Shen, D.; Cai, X. High durability of Pt-Ni-Ir/C ternary catalyst of PEMFC by stepwise reduction synthesis. *Electrochim. Acta* **2019**, *330*, 135251. [CrossRef]
129. Zhu, F.; Luo, L.; Wu, A.; Wang, C.; Cheng, X.; Shen, S.; Ke, C.; Yang, H.; Zhang, J. Improving the High-Current-Density Performance of PEMFC through Much Enhanced Utilization of Platinum Electrocatalysts on Carbon. *ACS Appl. Mater. Interfaces* **2020**, *12*, 26076–26083. [CrossRef] [PubMed]
130. Kim, J.; Kim, S.-I.; Jo, S.G.; Hong, N.E.; Ye, B.; Lee, S.; Dow, H.S.; Lee, D.H.; Lee, J.W. Enhanced activity and durability of Pt nanoparticles supported on reduced graphene oxide for oxygen reduction catalysts of proton exchange membrane fuel cells. *Catal. Today* **2019**, *352*, 10–17. [CrossRef]
131. Esfahani, R.A.M.; Easton, E.B. Exceptionally durable Pt/TOMS catalysts for fuel cells. *Appl. Catal. B Environ.* **2020**, *268*, 118743. [CrossRef]
132. Xu, C.; Fan, C.; Zhang, X.; Chen, H.; Liu, X.; Fu, Z.; Wang, R.; Hong, T.; Cheng, J. MXene ($Ti_3C_2T_x$) and Carbon Nanotube Hybrid-Supported Platinum Catalysts for the High-Performance Oxygen Reduction Reaction in PEMFC. *ACS Appl. Mater. Interfaces* **2020**, *12*, 19539–19546. [CrossRef]
133. Wang, R.; Chang, Z.; Fang, Z.; Xiao, T.; Zhu, Z.; Ye, B.; Xu, C.; Cheng, J. Pt nanowire/Ti3C2Tx-CNT hybrids catalysts for the high performance oxygen reduction reaction for high temperature PEMFC. *Int. J. Hydrogen Energy* **2020**, *45*, 28190–28195. [CrossRef]
134. Wei, L.; Shi, J.; Cheng, G.; Lu, L.; Xu, H.; Li, Y. Pt/TiN–TiO_2 catalyst preparation and its performance in oxygen reduction reaction. *J. Power Sources* **2020**, *454*, 227934. [CrossRef]
135. Devrim, Y.; Arıca, E.D. Investigation of the effect of graphitized carbon nanotube catalyst support for high temperature PEM fuel cells. *Int. J. Hydrogen Energy* **2019**, *45*, 3609–3617. [CrossRef]
136. Chu, T.; Xie, M.; Yang, D.; Ming, P.; Li, B.; Zhang, C. Highly active and durable carbon support Pt-rare earth catalyst for proton exchange membrane fuel cell. *Int. J. Hydrogen Energy* **2020**, *45*, 27291–27298. [CrossRef]
137. Tetteh, E.B.; Lee, H.-Y.; Shin, C.-H.; Kim, S.-H.; Ham, H.C.; Tran, T.-N.; Jang, J.-H.; Yoo, S.J.; Yu, J.-S. New PtMg Alloy with Durable Electrocatalytic Performance for Oxygen Reduction Reaction in Proton Exchange Membrane Fuel Cell. *ACS Energy Lett.* **2020**, *5*, 1601–1609. [CrossRef]
138. Wang, F.; Zhang, Q.; Rui, Z.; Li, J.; Liu, J. High-Loading Pt–Co/C Catalyst with Enhanced Durability toward the Oxygen Reduction Reaction through Surface Au Modification. *ACS Appl. Mater. Interfaces* **2020**, *12*, 30381–30389. [CrossRef]
139. Lin, R.; Zheng, T.; Chen, L.; Wang, H.; Cai, X.; Sun, Y.; Hao, Z. Anchored Pt-Co Nanoparticles on Honeycombed Graphene as Highly Durable Catalysts for the Oxygen Reduction Reaction. *ACS Appl. Mater. Interfaces* **2021**, *13*, 34397–34409. [CrossRef] [PubMed]
140. Ji, Z.; Perez-Page, M.; Chen, J.; Rodriguez, R.G.; Cai, R.; Haigh, S.J.; Holmes, S.M. A structured catalyst support combining electrochemically exfoliated graphene oxide and carbon black for enhanced performance and durability in low-temperature hydrogen fuel cells. *Energy* **2021**, *226*, 120318. [CrossRef]
141. Islam, J.; Kim, S.-K.; Kim, K.-H.; Lee, E.; Park, G.-G. Enhanced durability of Pt/C catalyst by coating carbon black with silica for oxygen reduction reaction. *Int. J. Hydrogen Energy* **2020**, *46*, 1133–1143. [CrossRef]
142. Gu, K.; Kim, E.J.; Sharma, S.; Sharma, P.R.; Bliznakov, S.; Hsiao, B.S.; Rafailovich, M.H. Mesoporous carbon aerogel with tunable porosity as the catalyst support for enhanced proton-exchange membrane fuel cell performance. *Mater. Today Energy* **2020**, *19*, 100560. [CrossRef]
143. Eren, E.O.; Ozkan, N.; Devrim, Y. Polybenzimidazole-modified carbon nanotubes as a support material for platinum-based high-temperature proton exchange membrane fuel cell electrocatalysts. *Int. J. Hydrogen Energy* **2020**, *46*, 29556–29567. [CrossRef]
144. Yang, X.; Zhang, G.; Du, L.; Zhang, J.; Chiang, F.-K.; Wen, Y.; Wang, X.; Wu, Y.; Chen, N.; Sun, S. PGM-Free Fe/N/C and Ultralow Loading Pt/C Hybrid Cathode Catalysts with Enhanced Stability and Activity in PEM Fuel Cells. *ACS Appl. Mater. Interfaces* **2020**, *12*, 13739–13749. [CrossRef] [PubMed]
145. Osmieri, L.; Park, J.; Cullen, D.A.; Zelenay, P.; Myers, D.J.; Neyerlin, K.C. Status and challenges for the application of platinum group metal-free catalysts in proton-exchange membrane fuel cells. *Curr. Opin. Electrochem.* **2021**, *25*, 100627. [CrossRef]
146. Zhan, Y.; Zeng, H.; Xie, F.; Zhang, H.; Zhang, W.; Jin, Y.; Zhang, Y.; Chen, J.; Meng, H. Templated growth of Fe/N/C catalyst on hierarchically porous carbon for oxygen reduction reaction in proton exchange membrane fuel cells. *J. Power Sources* **2019**, *431*, 31–39. [CrossRef]
147. Wan, X.; Liu, X.; Li, Y.; Yu, R.; Zheng, L.; Yan, W.; Wang, H.; Xu, M.; Shui, J. Fe–N–C electrocatalyst with dense active sites and efficient mass transport for high-performance proton exchange membrane fuel cells. *Nat. Catal.* **2019**, *2*, 259–268. [CrossRef]

148. Zhang, H.; Chung, H.T.; Cullen, D.A.; Wagner, S.; Kramm, U.I.; More, K.L.; Zelenay, P.; Wu, G. High-performance fuel cell cathodes exclusively containing atomically dispersed iron active sites. *Energy Environ. Sci.* **2019**, *12*, 2548–2558. [CrossRef]
149. Qiao, M.; Wang, Y.; Wang, Q.; Hu, G.; Mamat, X.; Zhang, S.; Wang, S. Hierarchically Ordered Porous Carbon with Atomically Dispersed FeN 4 for Ultraefficient Oxygen Reduction Reaction in Proton-Exchange Membrane Fuel Cells. *Angew. Chem.* **2019**, *132*, 2710–2716. [CrossRef]
150. He, Y.; Hwang, S.; Cullen, D.A.; Uddin, M.A.; Langhorst, L.; Li, B.; Karakalos, S.; Kropf, A.J.; Wegener, E.C.; Sokolowski, J.; et al. Highly active atomically dispersed CoN_4 fuel cell cathode catalysts derived from surfactant-assisted MOFs: Carbon-shell confinement strategy. *Energy Environ. Sci.* **2018**, *12*, 250–260. [CrossRef]
151. Yang, H.; Wang, X.; Zheng, T.; Cuello, N.C.; Goenaga, G.; Zawodzinski, T.A.; Tian, H.; Wright, J.T.; Meulenberg, R.W.; Wang, X.; et al. CrN-Encapsulated Hollow Cr-N-C Capsules Boosting Oxygen Reduction Catalysis in PEMFC. *CCS Chem.* **2021**, *3*, 208–218. [CrossRef]
152. Xie, X.; He, C.; Li, B.; He, Y.; Cullen, D.A.; Wegener, E.C.; Kropf, A.J.; Martinez, U.; Cheng, Y.; Engelhard, M.H.; et al. Performance enhancement and degradation mechanism identification of a single-atom Co–N–C catalyst for proton exchange membrane fuel cells. *Nat. Catal.* **2020**, *3*, 1044–1054. [CrossRef]
153. He, Y.; Guo, H.; Hwang, S.; Yang, X.; He, Z.; Braaten, J.; Karakalos, S.; Shan, W.; Wang, M.; Zhou, H.; et al. Single Cobalt Sites Dispersed in Hierarchically Porous Nanofiber Networks for Durable and High-Power PGM-Free Cathodes in Fuel Cells. *Adv. Mater.* **2020**, *32*, 2003577. [CrossRef]
154. Miao, Z.; Xia, Y.; Liang, J.; Xie, L.; Chen, S.; Li, S.; Wang, H.; Hu, S.; Han, J.; Li, Q. Constructing Co–N–C Catalyst via a Double Crosslinking Hydrogel Strategy for Enhanced Oxygen Reduction Catalysis in Fuel Cells. *Small* **2021**, *17*, 2100735. [CrossRef] [PubMed]
155. Chen, M.; Li, X.; Yang, F.; Li, B.; Stracensky, T.; Karakalos, S.; Mukerjee, S.; Jia, Q.; Su, D.; Wang, G.; et al. Atomically Dispersed MnN_4 Catalysts via Environmentally Benign Aqueous Synthesis for Oxygen Reduction: Mechanistic Understanding of Activity and Stability Improvements. *ACS Catal.* **2020**, *10*, 10523–10534. [CrossRef]
156. Luo, F.; Roy, A.; Silvioli, L.; Cullen, D.A.; Zitolo, A.; Sougrati, M.T.; Oguz, I.C.; Mineva, T.; Teschner, D.; Wagner, S.; et al. P-block single-metal-site tin/nitrogen-doped carbon fuel cell cathode catalyst for oxygen reduction reaction. *Nat. Mater.* **2020**, *19*, 1215–1223. [CrossRef]
157. Yang, X.; Wang, Y.; Zhang, G.; Du, L.; Yang, L.; Markiewicz, M.; Choi, J.-Y.; Chenitz, R.; Sun, S. SiO_2-Fe/N/C catalyst with enhanced mass transport in PEM fuel cells. *Appl. Catal. B Environ.* **2019**, *264*, 118523. [CrossRef]
158. Uddin, A.; Dunsmore, L.; Zhang, H.; Hu, L.; Wu, G.; Litster, S. High Power Density Platinum Group Metal-free Cathodes for Polymer Electrolyte Fuel Cells. *ACS Appl. Mater. Interfaces* **2019**, *12*, 2216–2224. [CrossRef]
159. Xu, J.; Liang, G.; Chen, D.; Li, Z.; Zhang, H.; Chen, J.; Xie, F.; Jin, Y.; Wang, N.; Meng, H. Iron and nitrogen doped carbon derived from ferrocene and ZIF-8 as proton exchange membrane fuel cell cathode catalyst. *Appl. Surf. Sci.* **2021**, *573*, 151607. [CrossRef]
160. Liu, S.; Meyer, Q.; Li, Y.; Zhao, T.; Su, Z.; Ching, K.; Zhao, C. Fe–N–C/Fe nanoparticle composite catalysts for the oxygen reduction reaction in proton exchange membrane fuel cells. *Chem. Commun.* **2022**, *58*, 2323–2326. [CrossRef]
161. Xie, X.; Shang, L.; Xiong, X.; Shi, R.; Zhang, T. Fe Single-Atom Catalysts on MOF-5 Derived Carbon for Efficient Oxygen Reduction Reaction in Proton Exchange Membrane Fuel Cells. *Adv. Energy Mater.* **2021**, *12*, 2102688. [CrossRef]
162. Zhu, W.; Pei, Y.; Douglin, J.C.; Zhang, J.; Zhao, H.; Xue, J.; Wang, Q.; Li, R.; Qin, Y.; Yin, Y.; et al. Multi-scale study on bifunctional Co/Fe–N–C cathode catalyst layers with high active site density for the oxygen reduction reaction. *Appl. Catal. B Environ.* **2021**, *299*, 120656. [CrossRef]
163. Cheng, Y.; Zhang, J.; Wu, X.; Tang, C.; Yang, S.-Z.; Su, P.; Thomsen, L.; Zhao, F.; Lu, S.; Liu, J.; et al. A template-free method to synthesis high density iron single atoms anchored on carbon nanotubes for high temperature polymer electrolyte membrane fuel cells. *Nano Energy* **2020**, *80*, 105534. [CrossRef]
164. Lee, S.W.; Lee, B.; Baik, C.; Kim, T.-Y.; Pak, C. Multifunctional Ir–Ru alloy catalysts for reversal-tolerant anodes of polymer electrolyte membrane fuel cells. *J. Mater. Sci. Technol.* **2020**, *60*, 105–112. [CrossRef]
165. Zhu, M.; Zhao, C.; Liu, X.; Wang, X.; Zhou, F.; Wang, J.; Hu, Y.; Zhao, Y.; Yao, T.; Yang, L.-M.; et al. Single Atomic Cerium Sites with a High Coordination Number for Efficient Oxygen Reduction in Proton-Exchange Membrane Fuel Cells. *ACS Catal.* **2021**, *11*, 3923–3929. [CrossRef]